TECTONIC SIGNIFICANCE OF GEOPHYSICAL INVESTIGATIONS IN SOUTHWESTERN
SUMNER, JOHN RANDOLPH
ProQuest Dissertations and Theses; 1971; ProQuest Dissertations & Theses Global

72-11,675

SUMNER, John Randolph, 1944-
TECTONIC SIGNIFICANCE OF GEOPHYSICAL INVESTIGATIONS IN SOUTHWESTERN ARIZONA AND NORTHWESTERN SONORA, MEXICO, AT THE HEAD OF THE GULF OF CALIFORNIA.

Stanford University, Ph.D., 1971
Geophysics

University Microfilms, A XEROX Company, Ann Arbor, Michigan

THIS DISSERTATION HAS BEEN MICROFILMED EXACTLY AS RECEIVED.

Reproduced with permission of the copyright owner. Further reproduction prohibited without permission.

TECTONIC SIGNIFICANCE OF GEOPHYSICAL INVESTIGATIONS IN SOUTHWESTERN ARIZONA AND NORTHWESTERN SONORA, MEXICO, AT THE HEAD OF THE GULF OF CALIFORNIA

A DISSERTATION

SUBMITTED TO THE DEPARTMENT OF GEOPHYSICS

AND THE COMMITTEE ON GRADUATE STUDIES

OF STANFORD UNIVERSITY

IN PARTIAL FULFILLMENT OF THE REQUIREMENTS

FOR THE DEGREE OF

DOCTOR OF PHILOSOPHY

By

John Randolph Sumner

August 1971

Reproduced with permission of the copyright owner. Further reproduction prohibited without permission.

I certify that I have read this thesis and that in my opinion it is fully adequate, in scope and quality, as a dissertation for the degree of Doctor of Philosophy.

George A. Thompson
(Principal Advisor)

I certify that I have read this thesis and that in my opinion it is fully adequate, in scope and quality, as a dissertation for the degree of Doctor of Philosophy.

Robert L Karach

I certify that I have read this thesis and that in my opinion it is fully adequate, in scope and quality, as a dissertation for the degree of Doctor of Philosophy.

Allan Cox

I certify that I have read this thesis and that in my opinion it is fully adequate, in scope and quality, as a dissertation for the degree of Doctor of Philosophy.

Ben M. Page
(Geology)

Approved for the University Committee on Graduate Studies:

Dean of Graduate Studies

Reproduced with permission of the copyright owner. Further reproduction prohibited without permission.

PLEASE NOTE:

Some pages have indistinct print. Filmed as received.

UNIVERSITY MICROFILMS.

Reproduced with permission of the copyright owner. Further reproduction prohibited without permission.

ABSTRACT

To investigate the morphology of an incipient spreading center and associated transform faults, an aeromagnetic survey and gravity survey were made of the region at the head of the Gulf of California. The Salton Trough and Gulf of California have formed as two large plates of the earth's crust move diagonally apart relative to one another.

Reconnaissance geology of the area shows that the ranges, which trend northwesterly approximately parallel to the Salton Trough, contain biotite and hornblende schist, granitic gneisses, granitic rocks, and widely scattered mesa-forming volcanic rocks. The Sierra del Pinacate of Sonora is a Quaternary shield volcano composed of olivine basalt which covers over 1000 km^2 of the pre-Quaternary terrain.

The Bouguer anomaly map constructed from the gravity survey shows that anomalies range from -7 to -35 mgals over bedrock exposures to -40 to -55 mgals over the centers of alluvial basins. Interpretation of the gravity data shows that basins northeast of the Salton Trough trend northwesterly and are from 0.25 to 1.25 kms deep. No northeasterly trending grabens, which would locate a spreading center, were detected. The gravity anomaly over the deep sedimentary basin of the Salton Trough is not as low as expected because sediment densities increase with depth and because the crust is tectonically thinned.

In order to cover a large area and also detect northeasterly trending anomalies which might be associated with spreading, the aeromagnetic survey was flown on north-south lines 5 km apart and at 1.3 km barometric elevation. The total field, residual magnetic map constructed

Reproduced with permission of the copyright owner. Further reproduction prohibited without permission.

from the aeromagnetic survey ranges from 600γ over basalts and some gneisses to 50γ over deep alluvial basins.The magnetic anomalies reflect the structural grain of the area and trend predominately to the northwest. Measurements of susceptibilities and remanent magnetizations of rock samples provide constraints for geologic models constructed from magnetic profiles.

Interpretation of geophysical and geologic data indicates some 30 km of strike-slip offset across the area northeast of the Salton Trough with an accompanying 2 - 3 km of extension. From the magnetic data, there is a large step in the basement(~3 km) between the Salton Trough and the adjacent terrain to the northeast. Geophysical data also shows that extensive buried sheets of basalt occur in at least two of the basins in Arizona.

The region of subdued magnetic anomalies in the northern Gulf of California is due to either deeply buried continental crust or crust transitional between continental and oceanic which has a shallow depth (11 km) to the Curie isotherm. Comparison of the zone of subdued anomalies with other areas formed by spreading of the earth's crust suggests that an inherent geologic mechanism causes subdued magnetic anomalies during early stages of spreading.

Reproduced with permission of the copyright owner. Further reproduction prohibited without permission.

ACKNOWLEDGMENTS

A regional geophysical investigation such as the one described here not only entails the collection, reduction, and interpretation of different types of geophysical data, but also crosses international boundaries. It is the sort of investigation which requires help from many people. Consequently, I would like to express my thanks to all those who helped bring this investigation to fruition.

Without the help of my father, John S. Sumner, this investigation could not have been done as efficiently, and I doubt that it could have been done at all. He provided his services as pilot and mentor beyond anything expected of kinship. To him I am most grateful.

A Penrose grant from the Geological Society of America covered flight costs for the aeromagnetic survey and Richard J. Wold kindly loaned the use of a magnetometer. Diego A. Córdoba and Guillermo P. Salas smoothed affairs on the international front by arranging for permission to fly over Mexican territory and providing location maps for the survey. William A. Sauck helped by passing on his experience and thoughts about aeromagnetic surveys and construction of magnetic maps.

I would like to thank Sam Stewart, Rob Wesson, and Tom Landers for initiating me into the wonders of data manipulation and reduction. John Cady kindly let me use his two-dimensional modeling program and Robert West loaned me his gravity data for southwestern Arizona.

I would also like to thank George Thompson for hundreds of helpful comments on data interpretation and minimization of verbal incrustations. I am grateful to Kathleen Hart for typing the bulk of the dissertation.

Reproduced with permission of the copyright owner. Further reproduction prohibited without permission.

To my wife Linda I am most indebted and grateful. She manipulated altimeter, magnetometer, keypunch, and typewriter with equal aplomb. Her calm through collisions with cattle, melted distributor points, and incomprehensible computer output gave sanity and security to the whole operation.

Reproduced with permission of the copyright owner. Further reproduction prohibited without permission.

TABLE OF CONTENTS

ABSTRACT		iii
ACKNOWLEDGMENTS		v
LIST OF ILLUSTRATIONS		viii
LIST OF TABLES		x
I.	INTRODUCTION	1
	1. PLATE MOTIONS	1
	2. PURPOSE AND SCOPE	9
II.	GEOLOGY	12
III.	GEOPHYSICAL DATA	19
	1. GRAVITY	19
	2. MAGNETICS	25
	Data Collection	25
	Magnetizations	34
	Brief Description of Aeromagnetic Map	43
	Anomaly Trends	44
	Geologic Model Cross Sections From Aeromagnetic Profiles	48
IV.	DISCUSSION	56
	1. STRUCTURAL FEATURES	56
	2. SUBDUED MAGNETIC ANOMALIES	63
V.	CONCLUSIONS	74
BIBLIOGRAPHY		77
APPENDIX		
	A. GRAVITY STATIONS	82

Reproduced with permission of the copyright owner. Further reproduction prohibited without permission.

LIST OF ILLUSTRATIONS

Figure		Page
1.	Simplified configuration of boundary between American and Pacific plates in western North America....	2
2.	Tectonic features of western North America.....	4
3.	Index map containing tectonic features and earthquake epicenters.....	7
4.	Location of rhombochasms and transform faults in the Gulf of California.....	10
5.	Regional geologic map of southwestern Arizona and northwestern Sonora.....	14
6.	Bouguer gravity map of the region at the head of the Gulf of California.....	22
7.	Gravity profiles and model geologic sections for profiles 1, 2, and 3 of figure 6.....	26
8.	Gravity profiles and model geologic sections for profiles 4, 5, 6, and 7 of figure 6.....	27
9.	Gravity profiles and model geologic sections for profiles 8 and 9 of figure 6.....	28
10.	Gravity profiles and model geologic sections for profiles 10 and 11 of figure 6.....	29
11.	Proton magnetometer and interfacing unit.....	30
12.	Location camera.....	32
13.	Flow chart for collection and reduction of aeromagnetic data.....	33
14.	Total field, residual magnetic map contoured on a 20-gamma interval.....	35
15.	Induced magnetizations for extusive rock samples....	36
16.	Induced magnetizations for granitic, gneissic, and metamorphic rocks.....	37
17.	Magnetic profiles over Sierra Hornaday.....	41

Reproduced with permission of the copyright owner. Further reproduction prohibited without permission.

Figure		Page
18.	Magnetic anomaly from a triangular element - used to determine magnetization of gneiss making up Sierra Hornaday	42
19.	Primary magnetic trends (closed highs and lows) for northwestern Sonora and southwestern Arizona	45
20.	Mineral and lithologic trends in the Cardigan gneiss (PreCambrian?) of the Ajo area	47
21.	Location of aeromagnetic profiles used to construct model geologic sections	49
22.	Magnetic profile and model geologic section for profile 1 of figure 21	52
23.	Magnetic profile and model geologic section for profile 2 of figure 21	53
24.	Magnetic profile and model geologic section for profile 3 of figure 21	54
25.	Magnetic profile and model geologic section for profile 4 of figure 21	55
26.	Structural and lithologic features found using geophysical techniques	58
27.	Simplified configuration of strike-slip deformation in the crystalline basement	60
28.	Magnetic profile and model geologic sections over zone of subdued magnetic anomalies in the northern Gulf of California	67
29.	Regions of subdued and large amplitude magnetic anomalies in the Red Sea and Gulf of California	70
30.	Magnetic profiles located in figure 29	71
31.	Wavelength and amplitude of magnetic anomalies over crust transitional between continental and oceanic in a region of spreading	73

Reproduced with permission of the copyright owner. Further reproduction prohibited without permission.

LIST OF TABLES

Table		Page
1.	Compilation of measured rock densities.....	23
2.	Remanent magnetizations for different demagnetizations and induced magnetizations for some intrusive and extrusive rocks.....	38
3.	Direction of remanent magnetizations for basalt samples.	40
4.	Induced and remanent magnetizations for major rock units.....	51
5.	Strike-slip offset on major faults in the Salton Trough and southwestern Arizona.....	62
6.	Thermal conductivities of selected earth materials.....	65

Reproduced with permission of the copyright owner. Further reproduction prohibited without permission.

I. INTRODUCTION

1. PLATE MOTIONS

The following hypotheses have been proposed to explain the formation of the Gulf of California: 1) Downfaulting along the axis of the Gulf, 2) emergence of Baja California with an elongate syncline forming the Gulf, 3) strike-slip movement on large strike-slip faults, 4) cross-strike movement of Baja California away from the Mexican mainland. On the basis of geophysical (Phillips, 1964; Harrison and Mathur, 1964) and geological (Allison, 1964) evidence, the first two hypotheses can be rejected. The Gulf of California has formed as the result of both strike-slip and cross-strike movement of Baja California relative to the Mexican mainland.

Applications of the theory of sea floor spreading and plate tectonics to western North America by Vine (1966), Morgan (1968), McKenzie and Morgan (1969), and Atwater (1970) indicate that Baja California and southern California southwest of the San Andreas fault system are moving northwesterly at about 6 cm per year with respect to the rest of the continent. The Gulf of California tectonic trough lies between the two plates. Following the terminology of Morgan (1968), Baja California and southern California southwest of the San Andreas fault system are now part of the Pacific plate and the rest of North America is part of the American plate. Figure 1 shows the simplified configuration of the two plates.

Atwater has modified the concept of a sharp boundary between the two plates by proposing that Cenozoic deformation in Oregon, Washington, Idaho, and the Basin and Range province of California, Nevada, Arizona, and Sonora represents a very wide, soft boundary between

Reproduced with permission of the copyright owner. Further reproduction prohibited without permission.

Reproduced with permission of the copyright owner. Further reproduction prohibited without permission.

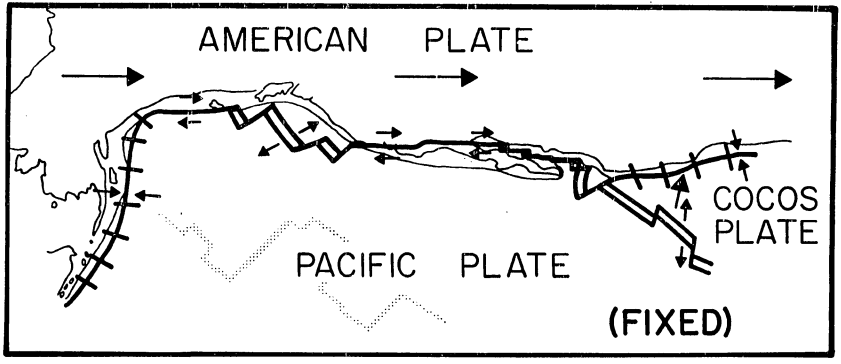

Figure 1. Simplified present configuration of plate boundaries in western North America and northeast Pacific, after Atwater (1970) and Morgan (1968). The map is a Mercator projection about the pole of relative motion between American and Pacific plates, 53°N, 53°W. Transform faults between the two plates form horizontal lines. Large arrows indicate plate motion of the American plate relative to the Pacific plate; small arrows indicate motion along boundaries between plates.

two rigid, moving plates. Figure 2 shows many of the significant tectonic features of western North America plotted on the same Mercator projection as figure 1.

From figure 2, Arizona and Sonora lie within the region of deformation between the two plates; consequently, faults in this area that are horizonaal on the Atwater projection tend to have pure strike-slip deformation and those oblique to the horizontal, extensional or compressional components of deformation.

Magnetic anomalies described by Larson and others (1968) at the mouth of the Gulf of California indicate that spreading in the Gulf started about four million years ago and that the Gulf is now spreading at a rate of 6 cm/yr. There is also good evidence (Moore and Buffington, 1968) that a proto-Gulf existed from Miocene time at the site of the present day Gulf of California.

The spreading or dilation within the Gulf itself appears greater in the southern half than the northern half (Rusnak and others, 1964). This disparity in apparent spreading indicates that extensional deformation in the northern Gulf occurs not only within the Gulf but also in the land surrounding the Gulf. Referring to figure 2, this means that north of 25°N, faults in Sonora to the east of the Gulf must take up the extensional deformation "missing" in the northern Gulf.

Oceanic spreading centers as described by Vine (1966) and Larson and others (1968) are broad, topographic highs or rises in the ocean floor which have a median trough running down their axis. Associated with the rises are large linear magnetic anomalies (>500γ) which parallel the spreading axis. Bouguer anomalies over the oceanic rises have values of about + 200 mgal and are about 100 mgals less than those

Reproduced with permission of the copyright owner. Further reproduction prohibited without permission.

Reproduced with permission of the copyright owner. Further reproduction prohibited without permission.

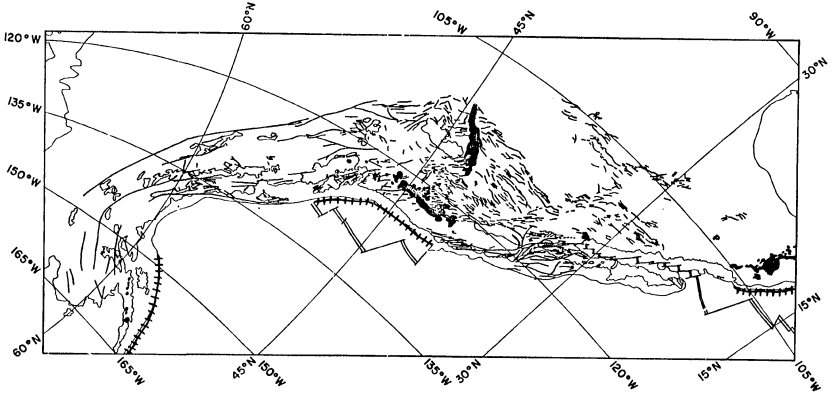

Figure 2. Tectonic features of North America (after King, 1969) plotted on same projection as Figure 1 (from Atwater, 1970). Quaternary volcanics are black; granitic plutons are gray; most thrust faults have been omitted. Horizontal faults experience pure strike slip; oblique faults have corresponding compression or rifting components.

found over the rest of the ocean floor.

From Larson and Speiss (1969), the East Pacific Rise at the mouth of the Gulf of California is a typical oceanic spreading center having a broad topographic high on the ocean floor and large linear magnetic anomalies (500γ-1000γ) parallel to the spreading axis. There is also a +200 mgal Bouguer anomaly over the East Pacific Rise at the mouth of the Gulf (Harrison and Mather, 1964). Lack of older oceanic crust on either side of the Rise in this area explains the lack of larger, positive Bouguer anomalies beyond the flanks of the Rise.

Within the Gulf of California, the spreading centers of the East Pacific Rise gradually lose their classic oceanic character for each succeeding segment up the Gulf. Broadly speaking, the nature of the spreading centers differs between the southern Gulf (below 28°N) and the northern Gulf and Salton Trough.

In the southern Gulf, spreading centers are different than those found in the deep ocean, but they are siill easily identified as such. Magnetic anomalies associated with the spreading centers are no longer linear, but are still large (200γ-500γ) (Larson and others, 1970). Bouguer gravity anomalies are still large, positive (+80 to +120 mgal), and centered over the spreading centers (Harrison and Mathur, 1964). In addition, each spreading center is a distinct bathymetric deep (Rusnak and others, 1964). From these data and from seismic refraction work by Phillips (1964), it may be concluded that oceanic crust less than four million years old forms the floor of the spreading centers in the southern Gulf.

In the northern Gulf, the truly awesome (4-6 km deep) sedimentary deposits of the Colorado River Delta obscure and complicate

Reproduced with permission of the copyright owner. Further reproduction prohibited without permission.

the features of the spreading centers. Bathymetric expressions become obliterated and kilometers of low density sediments influence the gravity anomalies and mask the magnetic features. Magnetic anomalies are small (~100γ) and broad and in no way indicative of a spreading center. Bouguer gravity anomalies are negative, but gentle highs may mark thinned continental crust or basaltic intrusion associated with spreading centers. The bathymetry is mostly non-distinctive, but small enclosed basins correlate well with the subdued gravity highs and most surely mark spreading centers. Thus, the northern Gulf and Salton Trough must also have distinctive areas of spreading, but these are not at all as well-defined as those in the southern Gulf due to the masking influence of the thick sediments of the Colorado River delta.

The seismicity in the northern Gulf and Salton Trough confirms the presence of spreading centers and transform faults and also locates ones which are presently active. Sykes (1967) has shown that the two principle mechanisms inherent to the ocean ridge system are (1) strike-slip motion on steeply dipping planes and (2) large component of normal faulting with the inferred tensional axis in the direction of spreading. Sykes (1970) has also shown that earthquake swarms arise from zones of extension such as spreading centers or areas of volcanic activity rather than zones of transform faulting.

An intense earthquake swarm in the northern Gulf in late March, 1969, was centered near 31°12'N, 114°31'W (Thatcher, 1970). Thatcher and Brune (1971) consider this earthquake swarm to be associated with a spreading center. Figure 3 shows the location of earthquake epicenters in the northern Gulf from the monthly

Reproduced with permission of the copyright owner. Further reproduction prohibited without permission.

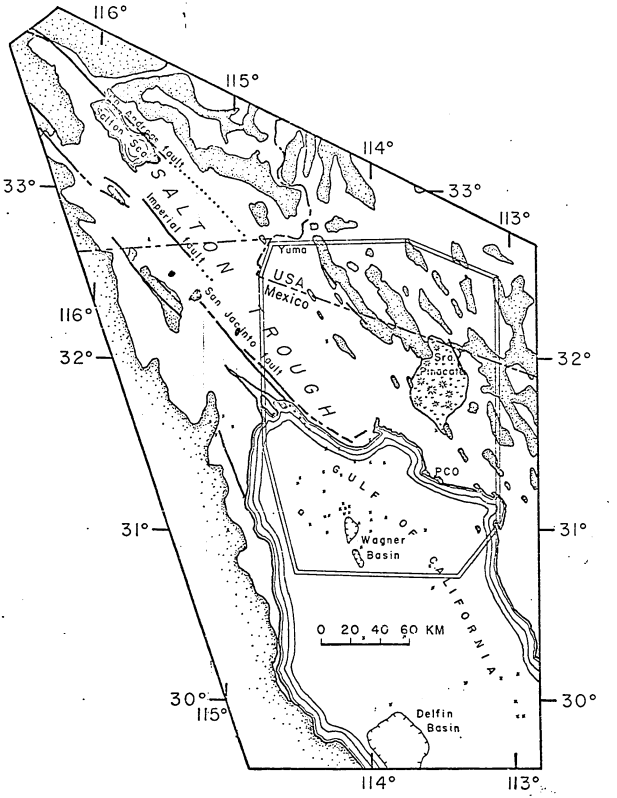

Figure 3. Index map showing tectonic features and area of investigation of the region at the head of the Gulf of California. Stippling marks pre-Quaternary crystalline basement, solid areas are known geothermal fields, heavy lines mark principle faults, v-pattern marks Quaternary lavas of the Sierra del Pinacate. Small x's mark epicentral locations (NOAA) from September, 1969 to March, 1971. The initials "PCO" mark the location of Puerto Penasco, Sonora.

Reproduced with permission of the copyright owner. Further reproduction prohibited without permission.

listing of epicenters by the National Oceanic and Atmospheric Administration.

In brief summary, the Gulf of California and Salton Trough represent a spreading zone between the Pacific and American plates. Seismic refraction, gravity, and magnetic data show that oceanic crustal material is present in the southern Gulf, indicating that spreading is more advanced in the southern Gulf than in the northern Gulf and Salton Trough or, at least, that it has shaken off the influence of adjacent continental blocks. The thin continental crust of the northern Gulf and Salton Trough indicates that the area is in an early stage of spreading and breakup of the continent.

The Salton tectonic trough can be considered the landward continuation of the Gulf of California tectonic trough. Work by Dibblee (1954) and Kovach and others (1962) shows that numerous northwesterly trending, parallel, strike-slip faults lie within the Salton Trough. Kovach and others (1962) present evidence that the San Jacinto fault is the most continuous of the strike-slip faults in the area but that the others are en echelon breaks related to it.

Two major and several minor geothermal areas lie within the Salton Trough. Fumaroles and rhyodacite cones of Quaternary age are associated with the Cerro Prieto geothermal field which has been described by Alonso-Espinosa and Mooser (1964) and Mercado (1969). Mud pots aligned along the trace of the San Andreas fault and transversely aligned rhyolite domes of Recent age mark the Salton geothermal field. Figure 3 shows the principle tectonic

Reproduced with permission of the copyright owner. Further reproduction prohibited without permission.

features of the Salton Trough.

2. PURPOSE AND SCOPE

In order to investigate tectonic deformation related to an incipient spreading center at the head of the Gulf of California, a geophysical investigation was made of the area shown in figure 3.

From investigations by previous workers (Kovach and others, 1962; Biehler and others, 1964), much is known about the thickness of the Cenozoic sediments, the configuration of the crystalline basement, and the location of strike-slip faults of the San Andreas system in the Salton Trough. However, it is not known how far the Salton Trough extends to the southeast, except that it does not reach the Mexican mainland. Instead the Trough must be offset in an en echelon manner to the southwest, in order to align itself with the Gulf Trough. One might look at the Salton tectonic trough as the last of the long string of spreading centers or tectonic "holes" which extend northwesterly from the mouth of the Gulf of California. Figure 4 shows how these spreading centers or rhombochasms are offset from each other in an en echelon manner on strike-slip or transform faults. The term "rhombochasm" is used here to describe a tectonically thinned part of the earth's crust. Thus under its semantic wing it includes spreading centers and tectonic troughs. As pointed out previously, the rhombochasms contain less than two kilometers of sedimentary fill in the southern Gulf, while in the northern Gulf and Salton Trough they are filled with over five kilometers of Pliocene and younger sediments of the Colorado River delta. Consequently, rhombochasms and their

Reproduced with permission of the copyright owner. Further reproduction prohibited without permission.

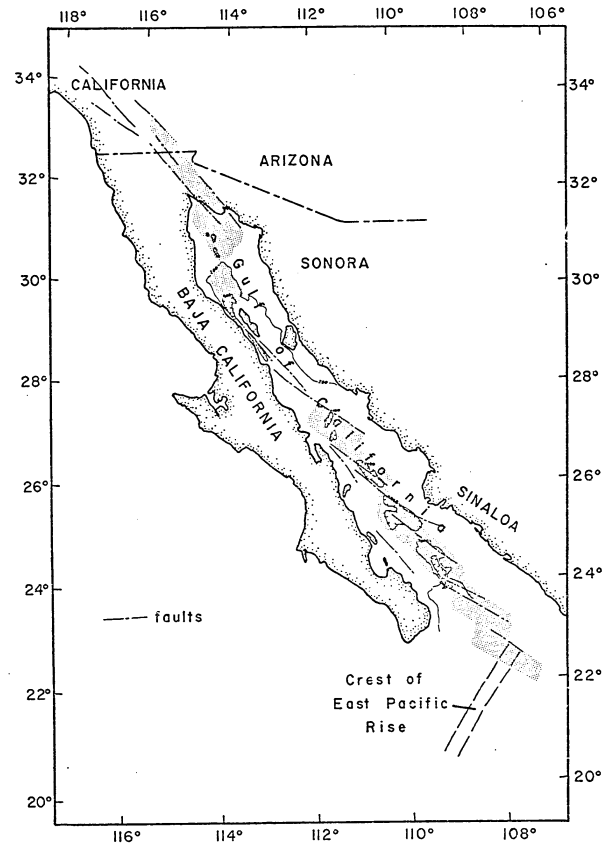

Figure 4. Rhombochasms (stippled areas) and transform faults within the Gulf of California. Rhombochasms coincide with basins, based on bathymetry from Rusnak and others (1964).

Reproduced with permission of the copyright owner. Further reproduction prohibited without permission.

transform faults in the northern Gulf region must be located using geophysical techniques.

As shown in figure 3, strike-slip faults of the San Andreas, Imperial, and San Jacinto fault system have been traced toward and into the area at the head of the Gulf. They do not continue on into Mexico east of the Gulf so they must terminate within the area and the motion must be taken up by parallel faults to the southwest. As with the Salton Trough, these new faults must form the structural control for the next rhombochasm down the Gulf.

If one looks at the system of rhombochasms in the simplest possible way, they would appear as a series of rectangular holes or depressions in the continental crust which are connected to one another by strike-slip faults. In reality the faulting is certainly more complex than this because of pre-rifting structural trends and the general inhomogeneous character of the continental crust.

The Pinacate volcanic field, which is here considered Quaternary in age because it has a fresh appearance and has no reversely magnetized flows, lies near the inferred southeastern boundary of the Salton Trough. It undoubtedly erupted as a result of tectonic activity associated with formation of the Salton Trough. No faults cut the flows of the Pinacate field, but volcanic explosion and collapse depressions up to two kilometers across appear to lie along pre-Pinacate structural trends.

That part of northwestern Sonora which lies at the head of the Gulf appears to be the site of an incipient spreading center. The present investigation aims to determine the extent of this spreading center or rhombochasm to the southeast, to locate faults

Reproduced with permission of the copyright owner. Further reproduction prohibited without permission.

which extend from the Salton Trough and Colorado River delta area, and to locate the next spreading center down in the Gulf. It was also hoped that the investigation would show whether or not the area adjacent to the Salton rhombochasm in Sonora and Arizona has undergone deformation related to formation of the Gulf and Salton tectonic troughs. In a more indirect way, there was the opportunity to compare the Salton Trough with similar extensional features such as the Red Sea.

Since the crystalline basement rocks are covered by sediments from 0.5 - 5 km thick over much of the area at the head of the Gulf, geophysical techniques are necessary to map the basement-sediment contact. Once the basement configuration is known, it is possible to locate the edge of the rhombochasm or trough and also the major faults within and adjacent to the rhombochasm.

Since this was a one-man operation and support funds were minimal, it was decided that a combination of regional gravity and aeromagnetic surveys would most efficiently determine the depth to crystalline basement and locate any major faults in the basement. I made a reconnaissance geologic map of the area as an aid in interpreting the aeromagnetic data and also to help determine the tectonic deformation of the geologic units in the area during formation of the Salton Trough.

In addition, I took samples of all major rock units within the area during the course of the gravity survey and while making field checks of the reconnaissance geologic map. I measured the densities and magnetization of these rock samples in order to properly interpret the gravity and aeromagnetic data.

Reproduced with permission of the copyright owner. Further reproduction prohibited without permission.

II. GEOLOGY

The area lies structurally within the broad zone of shearing and extension which has formed as the North American and Pacific plates move by one another. This broad tectonic zone contains the San Andreas and related strike-slip faults of the Salton Trough as well as the block fault features of much of western North America. Within the area of study, the mountain ranges trend parallel to the Salton Trough and to the major strike-slip faults in the trough. The shear deformation which has caused the strike-slip faults, has had a strong influence throughout the area. The northwesterly trending ranges in the area are bounded by strike-slip faults which have an additional normal component of faulting. The influence of structural trends older than the late Cenozoic deformation between the Pacific and North American plates has probably been overwhelmed by the recent tectonic activity racking the area.

Previous geologic work within the area has been primarily reconnaissance in nature, although the Ajo quadrangle mapped by Gilluly (1946) provides much of the stratigraphic information available for southwestern Arizona. Bryan (1923, 1925) and Wilson (1933) describe the metamorphic and intrusive rocks which make up the mountain ranges in south estern Arizona as: 1) biotite and hornblende schists, 2) granitic gneisses, and 3) granitic (to gabbroic) plutonic rocks. Similar schists, gneisses, and intrusive rocks make up all the ranges in northwestern Sonora with the exception of the Sierra del Pinacate, which is a Quaternary

Reproduced with permission of the copyright owner. Further reproduction prohibited without permission.

shield volcano of olivine basalt.

Wilson (1933) and Lord (1899) also describe andesitic extrusives in the Cabeza Prieta Mountains of Arizona and a basalt which forms widely scattered mesas in southwestern Arizona. With the exception of the Sierra del Pinacate, the crystalline "basement" complex makes up over 90% of the mountain ranges in the area.

The regional geologic map of figure 5 compiles geologic information as reported by Bryan (1925), Wilson (1933), Fries (1962), and a United Nations Development Programme report (1969) in addition to the writer's interpretation of air photos and field work.

The metamorphic rocks of figure 5 contain biotite and hornblende schists, granitic gneisses, and porphyritic granite gneiss. The schist occurs in contact with the gneiss in the Gila, Mohawk, and Cabeza Prieta Mountains in Arizona and in the Cerritos del Solito east of the Sierra del Pinacate in Sonora. The schist is locally altered by contact and hydrothermal metamorphism (Wilson, 1933). The granitic gneiss is far more widespread than the schist and occurs to some degree in every mountain range in the area.

The granitic rocks which intrude the metamorphic rocks are primarily biotite granites although there is a thin gabbro body which intrudes the granite in the Sierra del Tuseral and may be the intrusive counterpart of the mesa-forming basalt. The granitic rocks occur in a band, forty kilometers wide, centered along 32°20' N latitude. The granitic rocks occur in almost all the ranges in Arizona and about half the ranges in Sonora.

Three different volcanic extrusives represent periods of volcanism in Miocene(?), Pliocene(?), and Quaternary time respec-

Reproduced with permission of the copyright owner. Further reproduction prohibited without permission.

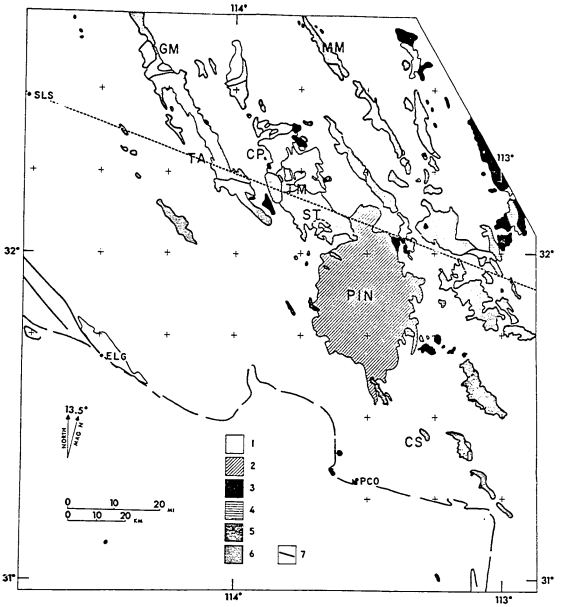

Figure 5. Regional geologic map of southwestern Arizona and northwestern Sonora. Explanation of symbols: 1 - Sedimentary rocks and alluvium; 2 - Pinacate basalt; 3 - Pliocene(?) basalt, typically forms mesas; 4 - Miocene(?) volcanics, intermediate to silicic composition; 5 - granitic rocks; 6 - schists and gneisses, Pre-Cambrian(?) age; 7 - Recent fault traces of the San Jacinto fault system. Place name symbols: SLS - San Luis del Rio Colorado; ELG - El Golfo de Santa Clara; PCO - Puerto Penasco; GM - Gila Mountains; PIN - Sierra del Pinacate; CP - Cabeza Prieta Mountains; MM - Mohawk Mountains; CS - Cerritos del Solito; ST - Sierra del Tuseral; TM - Tule Mountains; TA - Sierra Tinajas Altas (Tinajas Altas Mountains in Arizona).

Reproduced with permission of the copyright owner. Further reproduction prohibited without permission.

tively. The Miocene(?) volcanics are rhyolitic to andesitic in composition and occur as deeply eroded, tilted and faulted blocks. The Miocene(?) volcanics cover about 200 km^2 in the Tule Mountains and occur in Sonora as a few widely scattered hills east of the Sierra del Pinacate. There are no radiometric age dates for these rocks, but similarities in composition and deformation allow tentative correlations with (1) a thick sequence of rhyolitic to andesitic volcanics in the Ajo area and considered mid-Tertiary(?) in age by Gilluly (1946); (2) the mid-Miocene Alverson Canyon formation of the Imperial Valley (Dibblee, 1954); and (3) the mid-Miocene Comondu formation of Baja California (Beal, 1948). According to ideas presented by Lipman, Prostka, and Christiansen (1970) and Atwater (1970) these Miocene(?) volcanics represent the andesitic extrusion associated with an active trench which lay off the coast of North America in this area until 25 to 30 million years ago.

The Pliocene(?) volcanics are basaltic to basaltic andesite in composition and form widely scattered mesas throughout the area. These basalts are essentially flat-lying, but are cut by numerous northerly and northwesterly trending faults. This mesa-forming basalt, because of its composition and flat-lying-but-faulted nature, may be roughly contemporaneous with the Batamote andesite of the Ajo area (Gilluly, 1946) and possibly the early Pliocene Santa Rosa volcanics of California (Hawkins, 1970) and Truckhaven rhyolite of the Imperial Valley (Dibblee, 1954).

The olivine basalts of the Pinacate lava field are Quaternary in age. These basalts innundate some 1500 square kilometers of Sonora and Arizona in the form of a shield volcano. No faults have been found

Reproduced with permission of the copyright owner. Further reproduction prohibited without permission.

in the lava field but this may be due in part to the "healing" ability that an active volcano has to cover any of its wounds with fresh lava flows. Numerous cinder cones and craters, some up to 2 kms across mark the Pinacate lava field. The craters appear controlled by pre-existing structural features in the crystalline basement. It is possible that the Pinacate lavas are contemporaneous with the Tres Virgenes volcanics in the central Gulf (Wilson, 1948) and even the rhyodacite cones of the Cerro Prieto geothermal field south of Mexicali, but this is at best a risky correlation.

Sedimentary deposits ranging from sandstones and conglomerates to alluvial gravels fill the basins between ranges in Arizona and Sonora as well as the Salton tectonic trough. The basins in Arizona and Sonora are the result of strike-slip faults which have an additional component of normal faulting. These basins contain up to a kilometer of sediments. The Salton Trough is a more profound basin, formed by similar, but more extensive, strike-slip faulting and its associated normal offset. Kovach (1962) reports up to six kilometers of sediment in the Imperial Valley and Phillips (1964) finds a similar sedimentary thickness in the northern Gulf of California.

The mountain ranges, and their bounding faults, have a strong northwesterly trend very nearly paralleling the system of strike-slip faults in the Salton Trough. The faults of the Salton Trough trend 315° while the ranges trend 320-340°. However, tectonic activity in the area where the ranges are exposed is quiescent in comparison to the active rifting and faulting in the Salton Trough.

Reproduced with permission of the copyright owner. Further reproduction prohibited without permission.

The amazing similarity between the trend of the mountain ranges and strike-slip faults in the Salton Trough suggests that there is a common causal mechanism. If one assumes that strike-slip deformation parallels small circles about the pole of relative motion between the Pacific and American plates, then the relation between strike-slip and normal offset on any fault is:

$$ss = \int_0^z \frac{z \, dz}{\tan \theta \tan \phi}$$

where ss = strike-slip offset, z = vertical offset, θ = dip of fault, and ϕ = angle between fault trace and direction of small circle. This expression will be used later to examine the total amount of strike-slip offset in the area.

With the exception of the Pinacate lavas, all rocks in the area are faulted. Fault blocks in the Miocene(?) volcanics are tilted as much as 60° while fault blocks of the Pliocene(?) or mesa basalts are essentially flat lying or at most only slightly tilted. In the Ajo area (Gilluly, 1946) and in the Sierra Tinajas Altas of Sonora, conglomerates underlie the Miocene(?) volcanics, thus indicating a period of active faulting prior to or contemporaneous with extrusion of the older volcanics. Starting from mid-Tertiary(?) time, there were two periods of faulting which can be loosely associated with the periods of volcanism. The trend of the mid-Tertiary(?) faults is northerly. The Pliocene(?) faults, which are associated with inception of the Salton tectonic trough, trend 320°-345° and were responsible for forming the present day terrain of northwesterly elongate ranges.

Reproduced with permission of the copyright owner. Further reproduction prohibited without permission.

III. GEOPHYSICAL DATA

1. GRAVITY

A gravity survey consisting of 484 stations covers much of northwestern Sonora in the vicinity of the Sierra del Pinacate. These stations were tied to the Lukeville, Arizona, gravity base station (979340.43 mgals) established by Bhuyan (unpub.) in 1965 and modified by the Army Map Service in 1968. This station is in turn tied to the North American gravity base network station WA3 (Woollard and Rose, 1963) in Tucson, Arizona. I used LaCoste-Romberg gravity meters No. 176 and No. 102 to make the survey. Six base stations established in northwestern Sonora served to tie all stations into the World Wide gravity network. Instrument drift is negligible and the effect of tidal gravity is less than 0.3 mgals over six hours. In comparison, gravity errors of $\pm$ 1.3 mgals arise from the use of a barometric altimeter to determine elevations of many of the gravity stations. Consequently, the tidal gravity effect was neglected for all gravity stations with the exception of the six gravity base stations.

Station elevations had a considerable range of reliability. Station elevations at benchmarks established along Route 2 in Sonora by the Universidad Nacional Autonomica de México, Departamento de Geofísica are known to within 0.1 m (0.02 mgals). Station elevations at road junctions having spot elevations on the AMS sheets are known to within 2.0 m (0.4 mgals). Station elevations along the Gulf shoreline are known to within 1.0 m (0.2 mgals). In the broad, flat valleys east of the Sierra del Pinacate, station elevations were

Reproduced with permission of the copyright owner. Further reproduction prohibited without permission.

determined by interpolation between contour lines and are accurate to $\pm$ 3 m ($\pm$ 0.6 mgals). Station elevations within the Sierra del Pinacate and other ranges were found using a barometric altimeter and are accurate to $\pm$ 7 m ($\pm$ 1.4 mgals).

Even though the desert ranges of Sonora are all very rugged, they do not cover large areas and consequently do not cause severe terrain corrections. Terrain corrections exceed two mgals for only three stations through Hayford-Bowie zone J (outer radius = 12.4 kilometers). Over 95% of the stations have terrain corrections of less than one milligal through Hayford-Bowie zone J, and of these, 90% have terrain corrections of less than 0.25 milligals. For all stations, except those along Route 2 and the shoreline of the Gulf of California, the errors arising from elevation uncertainties exceed those arising from neglecting terrain corrections. As examples, stations in the valleys have elevations known to $\pm$ 3 m causing an error in the Bouguer anomaly of about $\pm$ 0.5 mgal -- and terrain corrections are always less than 0.25 mgal for valley stations. For mountain stations, elevations are known to $\pm$ 7 m causing an error of $\pm$ 1.3 mgal -- and terrain corrections are typically less than 1 mgal for mountain stations. Consequently, terrain corrections have been neglected.

Errors arising from location uncertainties are small compared to elevation error. All stations are locatable on the AMS sheets to 0.2 km, causing an error in the gravity of $\pm$ 0.1 mgal.

The average probable error for any gravity station can be expressed as a root mean square of the errors.

$$\text{Probable error} = \left[(\text{tidal errors})^2 + (\text{elevation errors})^2 + (\text{error from neglecting terrain correction})^2 + (\text{latitude error})^2 / \frac{(\text{errors})}{4} \right]^{1/2}$$

Reproduced with permission of the copyright owner. Further reproduction prohibited without permission.

For valley stations:

Probable error = $[(0.3)^2 + (0.5)^2 + (0.2)^2 + (0.1)^2/(\frac{1.1}{4})]^{1/2}$

$= \pm 1.26$ mgal.

For mountain stations:

Probable error = $[(0.3)^2 + (1.5)^2 + (1.0)^2 + (0.1)^2/(\frac{2.9}{4})]^{1/2}$

$= \pm 2.15$ mgals.

For stations along Route 2 and the shoreline of the Gulf of California, the probable error for an individual station is less than 0.3 mgal.

The Bouguer anomalies are plotted as an isogal map contoured with a 5 and 10 mgal contour interval. The Bouguer gravity map is shown in figure 6. The different symbols indicate the confidence level of the individual gravity station. Appendix A lists all the gravity stations.

Rock densities for the area at the head of the Gulf of California are shown in table 1. The densities for the sedimentary rocks include well hole samples from the Salton Trough (Kovach and others, 1962).

The major density units are: crystalline basement and basalt -- 2.65 to 2.70 gm/cc; intermediate to silicic volcanics -- 2.40 to 2.45 gm/cc; and alluvium and surface deposits -- 2.2 gm/cc (Thompson, 1958). For the deeper alluvial basins where considerable compaction has taken place, an average density of 2.4 gm/cc is assumed (Kovach and others, 1962).

From figure 6, it can be seen that the Bouguer gravity anomalies have a 55 mgal range. The anomaly values range from highs of -5 mgal and -7 mgal at bedrock exposures in the Mohawk mountains of Arizona and the Sierra Blanca of Sonora to lows of -50 mgal over the alluviated basins of the Tule, Lechuguilla and Yuma deserts; -55 mgal near the mouth of the Colorado River; and -60 mgal over areas of higher elevation along the eastern edges of the survey area. The Bouguer anomalies trend

Reproduced with permission of the copyright owner. Further reproduction prohibited without permission.

Reproduced with permission of the copyright owner. Further reproduction prohibited without permission.

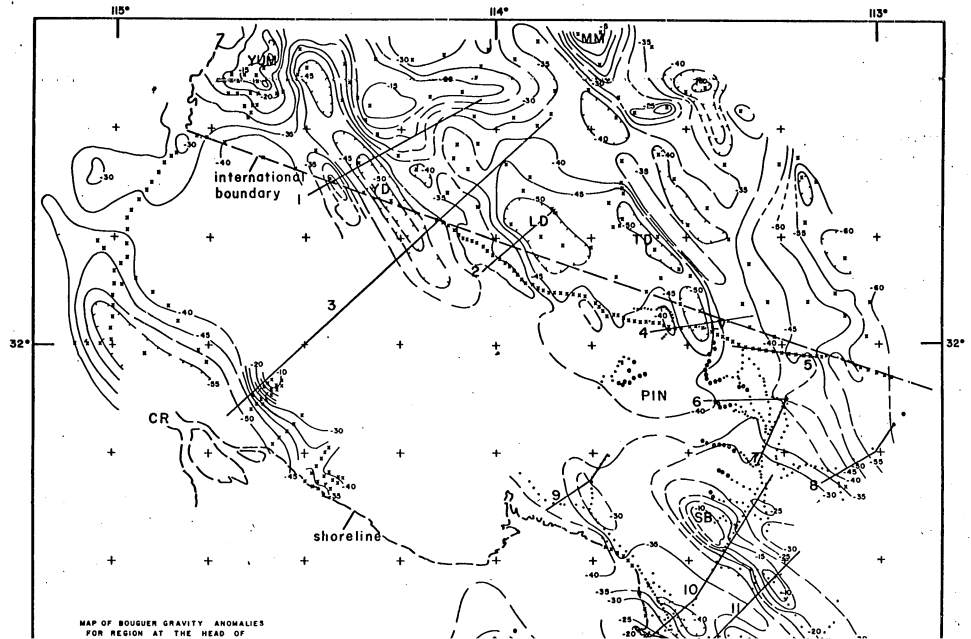

MAP OF BOUGUER GRAVITY ANOMALIES
FOR REGION AT THE HEAD OF

Reproduced with permission of the copyright owner. Further reproduction prohibited without permission.

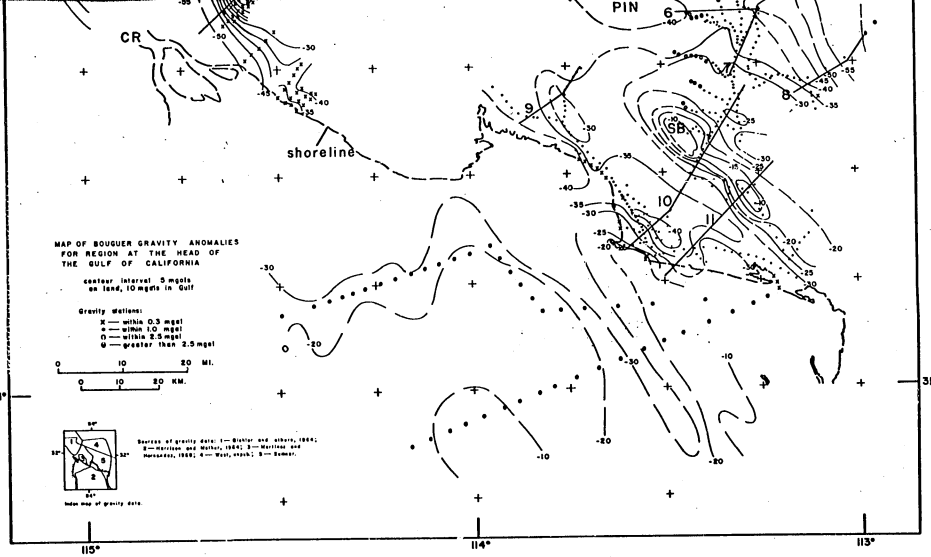

Figure 6. Bouguer gravity anomaly map for the region at the head of the Gulf of California. Numbered profiles are modeled in figures 7, 8, 9, and 10. Place names referred to in text: YUM - Yuma, Arizona; LV - Los Vidrios; CR - Colorado River mouth; MM - Mohawk Mountains; SB - Sierra Blanca; YD - Yuma Desert; LD - Lechuguilla Desert; TD - Tule Desert; PIN - Sierra del Pinacate.

TABLE 1

Samples	No. of Samples	Range of Measured Densities (gm/cc)	Average Density (gm/cc)
Granitic and gneissic rocks	13	2.58 - 2.72	2.61
Schist	3	2.71 - 2.95	2.82
Granite porphyry	3	2.63 - 2.73	2.66
Basalt (nonvesicular)	12	2.63 - 2.85	2.74
Rhyodacite and vesicular basalt	9	2.00 - 2.64	2.45
Sedimentary rocks (sandstone and coquina)	3	2.02 - 2.31	2.12
well samples (Kovach, 1962)			
0 - 1.3 km	8	2.06 - 2.66	2.37
1.3 - 2.6 km	15	2.23 - 2.57	2.44
2.6 - 4.0 km	4	2.35 - 2.59	2.47

TABLE 1. Measured wet rock densities from northwestern Sonora plus well samples (Kovach, 1962) from the Colorado River Delta.

Reproduced with permission of the copyright owner. Further reproduction prohibited without permission.

generally northwesterly, in reflection of the structural grain of the area. Gravity highs generally coincide with mountain ranges in the northeastern half of the area -- notable exceptions to this in Arizona may be due to the distance between stations or the lack of stations over bedrock areas.

The typical difference in the Bouguer anomaly between a mountain range and alluvial valley is -15 to -20 mgal. For a density contrast of 0.5 gm/cc between the crystalline basement rocks and the sedimentary deposits, the basin sediments are 750 to 1000 meters thick. The Bouguer anomaly differences between the crystalline basement rocks near Yuma and the area around the San Jacinto fault near the mouth of the Colorado River is -20 to -30 mgals. For a density contrast of 0.3 mgals between the basement rocks and sediments, the calculated depth to basement is 1600 to 2400 meters which does not agree with depth estimates from magnetic and seismic data (Phillips, 1964; Biehler and others, 1964). As pointed out by Kovach and others (1962), depth estimates in the Colorado Delta region from the gravity data are low compared to seismic and borehole data because the crust thins under the Salton Trough and also because density increases with depth in the sedimentary section and approaches the bedrock densities. Recent interpretation of gravity data by Biehler (1971) in the Salton Trough shows that the crust is thin (20 km) there and has a slightly higher density (0.1 gm/cc) than adjacent crust.

The long linear structures in the area lend themselves to two-dimensional modeling of various gravity anomalies. For the most part, gravity highs are associated with bedrock exposures or indicate a thinning of sediments. Similarly, gravity lows lie over the centers of alluvial basins. From the gravity data, estimates of sediment

Reproduced with permission of the copyright owner. Further reproduction prohibited without permission.

thicknesses indirectly indicate the amount of faulting and tilting of the basement rocks. Gravity profiles and model geologic cross-sections for the alluvial basins indicate that the deepest basins in the northeastern and eastern parts of the area are filled with about 1 km of sediments.

Figure 6 shows the location of several profiles modeled using computational techniques described by Talwani and others (1959). The scarcity of stations in Arizona limits modeling in these areas. In fact, conclusions drawn from the model profiles in Arizona must be considered tentative. The primary purpose of the model profiles is to determine the sediment thickness and as a consequence determine the location, size and extent of structural features. Information from gravity modeling with regard to the depth to basement and location of faults in the valleys puts a constraint on the models which will be used later in magnetic modeling. Figures 7,8, 9, and 10 show the various model profiles of figure 6.

2. MAGNETICS

Data collection

A Cessna 180 was used for the aeromagnetic survey. A GeoMetrics portable proton magnetometer, model G-806 was the heart of the airborne magnetometer system. The sensor was towed on a cable strung 30 meters behind the plane. The instrument had a one-gamma precision and a sampling rate of 2 seconds. An interfacing unit with an internal digital clock allowed simultaneous analog (Rustrak tape) and digital (BCD paper tape) output. Figure 11 shows the magnetometer and interface unit. Every 1, 5, or 50 magnetometer readings, depending on the survey requirements, the interfacing unit simultaneously punched

Reproduced with permission of the copyright owner. Further reproduction prohibited without permission.

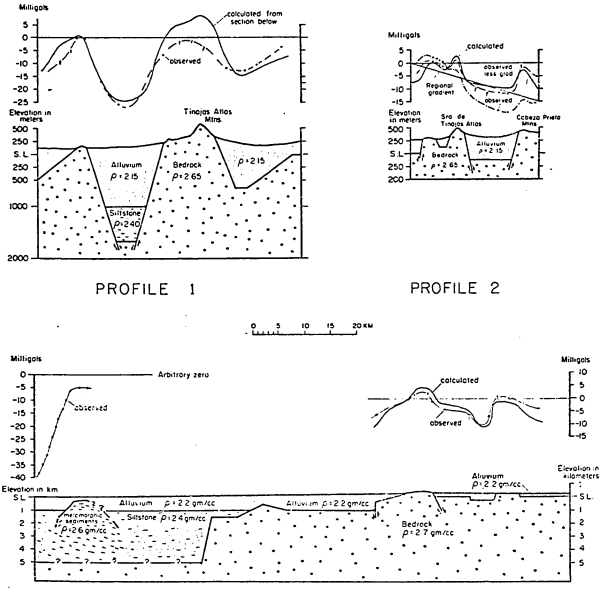

Figure 7. Gravity profiles and model geologic sections for profiles 1, 2, and 3 of Figure 6.

Reproduced with permission of the copyright owner. Further reproduction prohibited without permission.

Reproduced with permission of the copyright owner. Further reproduction prohibited without permission.

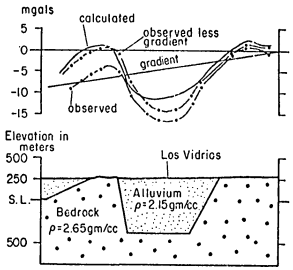

PROFILE 4

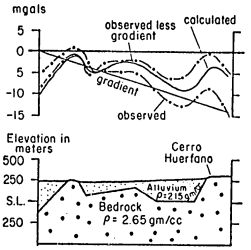

PROFILE 5

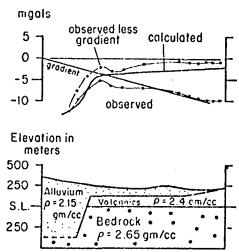

PROFILE 6

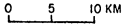

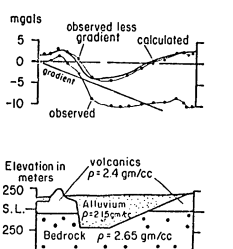

PROFILE 7

Figure 8. Gravity profiles and model geologic sections for profiles 4, 5, 6, and 7 of Figure 6.

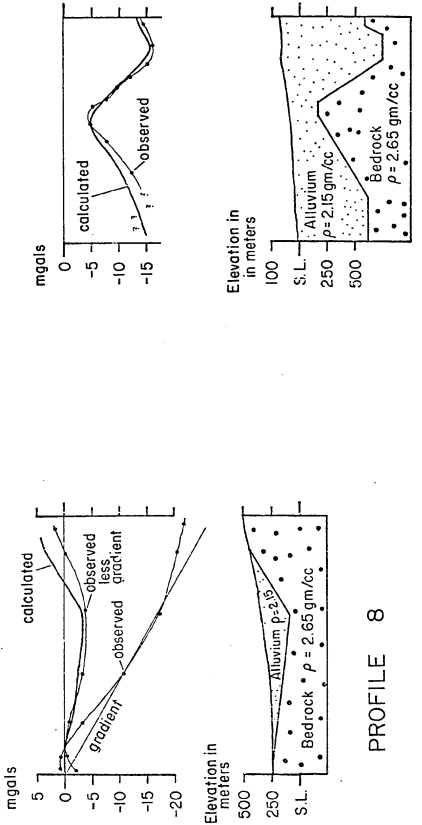

Figure 9. Gravity profiles and model geologic sections for profiles 8 and 9 of figure 6.

Reproduced with permission of the copyright owner. Further reproduction prohibited without permission.

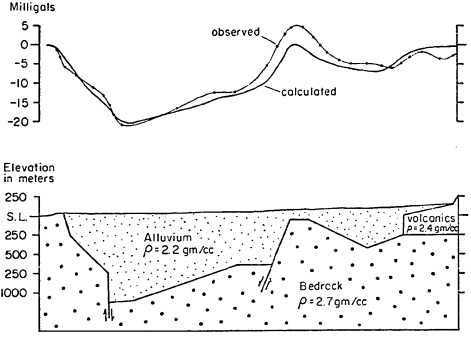

PROFILE 10

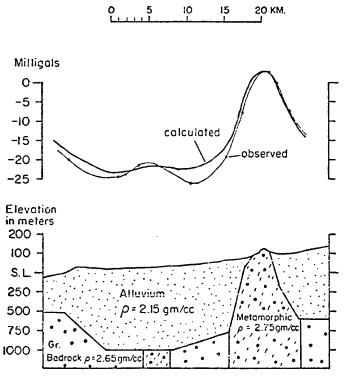

PROFILE 11

Figure 10. Gravity profiles and model geologic sections for profiles 10 and 11 of Figure 6.

Reproduced with permission of the copyright owner. Further reproduction prohibited without permission.

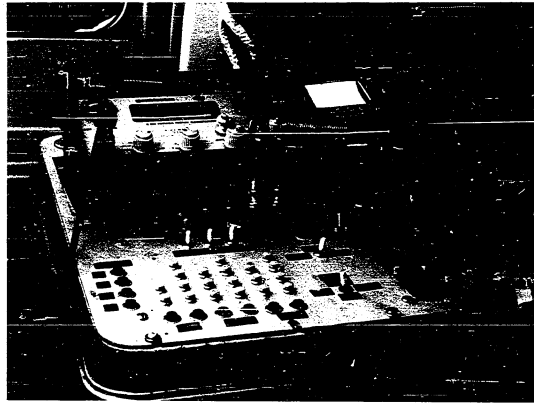

Figure 11. Proton magnetometer (GeoMetrics model G-806) and interfacing unit. The interfacing unit contains a digital clock, analog output, and digital output.

Reproduced with permission of the copyright owner. Further reproduction prohibited without permission.

the time on the digital output and triggered the location camera which was mounted on the floor of the airplane. The location camera (see figure 12) was a shock-mounted Beattie-Coleman Varitron, model D 9-68 with a data recording chamber. The data recording chamber contains a clock and frame counter -- a small prism between the data chamber and the film magazine allowed the time and frame number to be recorded on the side of each frame.

For a regional aeromagnetic survey of this sort, it was desired to cover a large area but with flight lines close enough together and low enough (the two are interdependent) so that there would be good correlation of isogamma contours between flight lines as well as a high sensitivity. The average elevation of the ground surface is 0.20 to 0.3 km (600 - 1000') with only a few widely scattered peaks as high as 1.0 km (3000'), and only the central peak of the Sierra del Pinacate is 1.3 km high (4000'). The structural grain of the area is northwesterly, but it was suspected that northeasterly trends might also be important. To detect both these trends with a high resolution, the aeromagnetic survey was flown on north-south lines 5 km apart at a barometric altitude of 1.3 km (4000'). Variations from the constant elevation were less than 100 meters. Flight lines over the Gulf of California were flown at 0.3 km (1000').

Diurnal magnetic variations measured at the Tucson observatory of the Coast and Geodetic Survey, 250 to 400 km from points in the survey area, were removed. Tie lines crossing the north-south lines dictated additional corrections to the magnetic base level to bring all flight lines to a common base. The International Geomagnetic Reference Field (Cain, 1969) was removed and 400 gammas added to yield positive gamma values. The generalized flow chart of figure 13 shows the various collection and

Reproduced with permission of the copyright owner. Further reproduction prohibited without permission.

Figure 12. Location camera mounted on the floor in the tail section of the airplane. The data recording chamber, which contains a clock and frame counter, is on the left. The film chamber is in the center, advance mechanism and external frame counter are on the right.

Reproduced with permission of the copyright owner. Further reproduction prohibited without permission.

Reproduced with permission of the copyright owner. Further reproduction prohibited without permission.

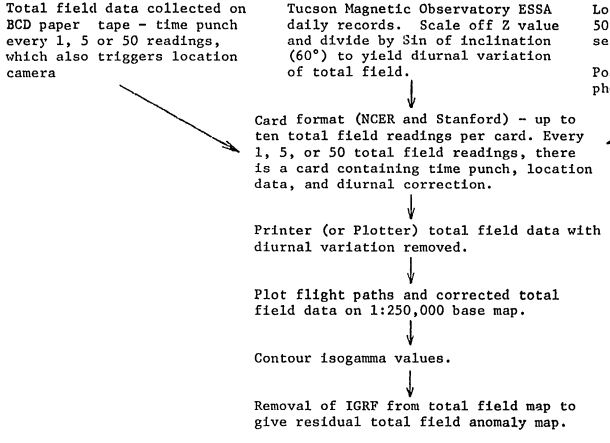

Figure 13. Flow chart for collection and reduction of aeromagnetic data.

reduction steps taken in making the final aeromagnetic map. The total field, residual aeromagnetic map is shown in figure 14. Errors between flight lines arise from instrument and magnetic noise ($\pm 5\gamma$), elevation inconsistancies ($\pm 10\gamma$), poor tie line control ($\pm 5\gamma$), and location errors ($\pm 15\gamma$). The probable error between any two flight lines may be expressed as a root mean square of the errors.

$$\text{Probable error} = \left[\left[(5)^2 + (5)^2 + (10)^2 + (15)^2\right] / \frac{5+5+10+15}{4}\right]^{1/2}$$

$$\text{Probable error} = \pm 6.5\gamma$$

For most of the survey area, this does not cause a significant deviation in contour lines. However, for the low gradient areas in the west central portion of the area, the error can amount to a deviation in the isogamma contours of several kilometers.

Magnetizations

To properly interpret the aeromagnetic map, it is necessary to know the magnetizations of all rock units within the area.

Susceptibilities of rock samples taken from all the major units were measured using a Soiltest, Inc. magnetic susceptibility bridge, model MS-3. The induced magnetizations for basaltic extrusives, silicic extrusives, granitic and gneissic rocks, metavolcanics, and schist are summarized in figures 15 and 16.

The remanent magnetizations of three of the granitic to gneissic rocks and the Miocene(?), Pliocene(?), and Pinacate extrusives were measured using a slow spinner magnetometer. To gauge the "hardness" of the remanent magnetizations, the samples were demagnetized in a 50-oersted field and the resulting remanent magnetization compared to the initial remanence. The results of these measurements are shown in table 2. For samples with soft magnetization (low coercivities),

Reproduced with permission of the copyright owner. Further reproduction prohibited without permission.

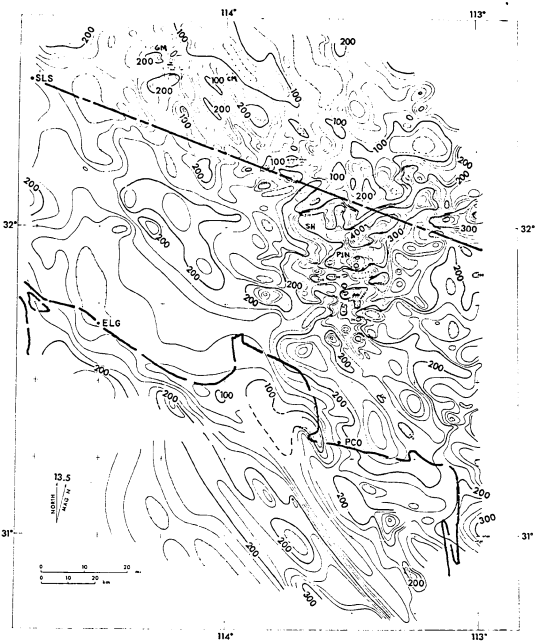

Figure 14. Total field, residual aeromagnetic map with a 20-gamma contour interval. International boundary between U.S. and Mexico is shown with a single dashed line, shoreline of the Gulf of California with a broken line. Place name symbols: SLS - San Luis del Rio Colorado; ELG - El Golfo de Santa Clara; PCO - Puerto Penasco; GM - Gila Mountains; CM - Copper Mountains; SH - Sierra Hornaday; PIN - Sierra del Pinacate.

Reproduced with permission of the copyright owner. Further reproduction prohibited without permission.

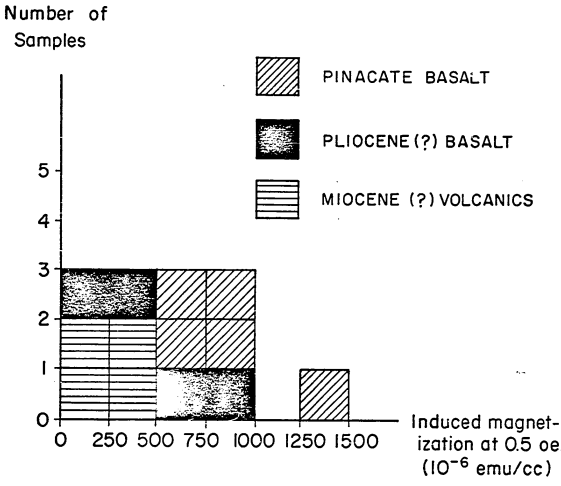

Figure 15. Induced magnetizations (0.5-oe. inducing field) for extrusive rock samples

Reproduced with permission of the copyright owner. Further reproduction prohibited without permission.

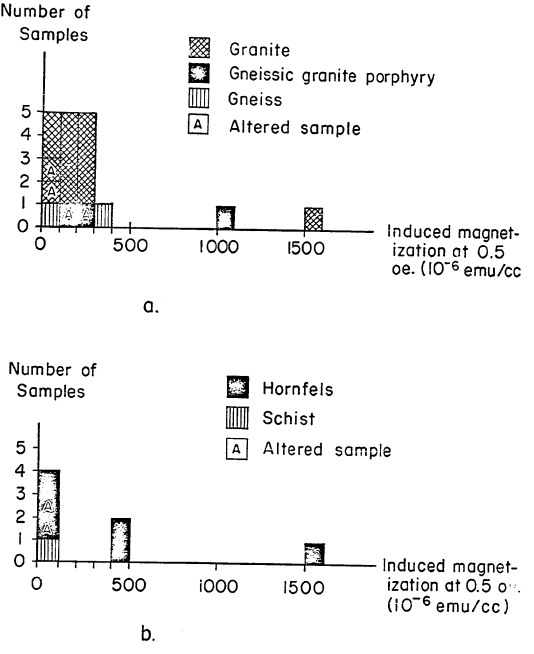

Figure 16. Induced magnetizations (0.5-oe. inducing field) for granitic, gneissic, and metamorphic rocks.

Reproduced with permission of the copyright owner. Further reproduction prohibited without permission.

TABLE 2

Sample	J_r ($\times 10^{-6}$ emu/cc) 0-oe demag	50-oe demag	100-oe demag	200-oe demag	J_i ($\times 10^{-6}$ emu/cc)
granite (#6)	149	41	--	--	190
porphyritic granite (#47)	254	167	--	--	~1000
biotite granite (#1)			--	--	209
Pliocene(?) basalt (LV1)	1200	840	428	246	201
Miocene(?) welded tuff (#5)	98.9	61.5	53.6	50.3	<20
Miocene(?) welded tuff (#1-5)	184	167	132	98	<20
Pinacate basalt (PT1)	4050	3730	--	--	~1000
Pinacate basalt (PT2)	2740	2580	--	--	780
Pliocene(?) basalt (BT1)	1370	370	260	--	~650

TABLE 2. Remanent magnetizations before and after demagnetizations and induced magnetizations (0.5-oersted field) for some intrusive and extrusive rocks.

Reproduced with permission of the copyright owner. Further reproduction prohibited without permission.

the intensity of the remanence should drop by at least half after a 50-oersted demagnetization. The granitic and gneissic rocks display soft remanent magnetization and the basalts have a somewhat harder remanence -- exactly as expected. The Q's (remanence/induced) for the intrusive rocks are less than or equal to one while Q's for the extrusive rocks are from two to six.

The direction of the remanent magnetization for the Pliocene(?) basalt and the Pinacate basalt at various demagnetizations are shown in table 3.

From the measurements of susceptibility and remanence of the extrusive and intrusive rocks, directions and intensities of magnetization can be assigned to the different rock units. These are used to interpret aeromagnetic profiles in a following section. Table 4 summarizes these results.

In places too inaccessible to collect a sample or where deep weathering prevented collection of a "clean" sample, it was possible to determine the magnetization by flying an aeromagentic profile at a low elevation over an area of known topography. The results of this technique for a low level aeromagnetic survey over the Sierra Hornaday of Sonora agree very well with results from samples.

Figure 17 shows the observed magnetic profiles over different parts of the Sierra Hornaday, a mountain range of granitic gneiss exposed in the northwestern part of the Pinacate lava field. These north-south profiles cross the backbone of the Sierra Hornaday at right angles. Some complications arise in the eastern profile from a thick basalt sheet south of the mountain. In spite of these complications, from the model curve over the triangular element of figure 18, which approximates the mountain range, it is possible to calculate

Reproduced with permission of the copyright owner. Further reproduction prohibited without permission.

TABLE 3

Sample	Inclination in degrees (demagnetizing field in oersteds)				Declination in degrees (demagnetizing field in oersteds)			
	I_0	I_{50}	I_{100}	I_{200}	D_0	D_{50}	D_{100}	D_{200}
Pliocene(?) basalt (LV1)	6	5	5	6	83	79	53	30
Pinacate basalt lightning struck (Fowler, pers. comm.)	-36	-36	-30	-25	49	48	55	57
Pliocene(?) basalt (BT1)	-30	-44	-47	--	47	48	120	--
Pinacate basalt (PT1)	39	42	--	--	9	2	--	--
Pinacate basalt (PT2)	39	38	--	--	-26	-16	--	--

TABLE 3. Direction of remanent magnetizations for some samples of Pliocene(?) basalt and Pinacate basalt. Demagnetizing fields up to 200 oersteds used.

Reproduced with permission of the copyright owner. Further reproduction prohibited without permission.

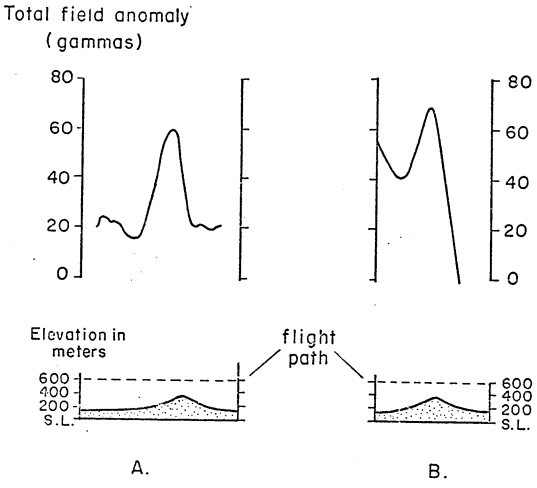

Figure 17. North-south aeromagnetic profiles over Sierra Hornaday. Peak to peak values used to calculate magnetization of gneiss making up Sierra Hornaday. A) western peak, B) eastern peak.

Reproduced with permission of the copyright owner. Further reproduction prohibited without permission.

Reproduced with permission of the copyright owner. Further reproduction prohibited without permission.

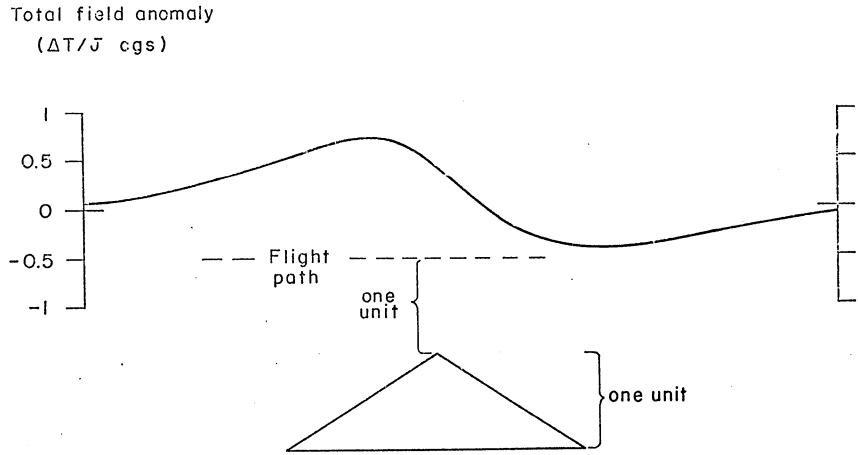

Figure 18. Magnetic anomaly over a triangular element. Used to determine magnetization of gneiss making up Sierra Hornaday.

the magnetization of the granitic gneiss making up the Sierra Hornaday. The peak to peak value of the normalized total field anomaly for the triangular body of figure 18 is 0.7. To find the magnetization, this value is divided into the observed peak to peak difference. For magnetic profile 1 of figure 19 the magnetization is

$$J_1 = \frac{30 \text{ to } 40 \times 10^{-5}}{0.7} \ \frac{\text{emu}}{\text{cc}} = 430 \text{ to } 570 \times 10^{-6} \text{ emu/cc}$$

and for profile 2 (figure 19)

$$J_2 = \frac{30 \times 10^{-5}}{0.7} \ \frac{\text{emu}}{\text{cc}} = 430 \times 10^{-6} \text{ emu/cc}$$

The magnetization determined from the second profile is possibly incorrect because a large gradient, probably due to a thick basalt body south of the mountain, makes it difficult to determine the base level of the anomaly due to the mountain.

Comparing these results with magnetizations of samples collected in the Sierra Hornaday shows a good agreement. The two samples collected have induced magnetizations of 113×10^{-6} emu/cc and 209×10^{-6} emu/cc. Assuming a Q of one for the grantic gneiss of the Sierra Hornaday, the sum of induced and remanent magnetization is from 225 to 420×10^{-6} emu/cc. The lower total magnetization measured in the surface samples could be due to surface weathering.

Brief description of aeromagnetic map

The aeromagnetic map of figure 14 shows a range of 500 gammas, from a 550 gamma high in the northern part of the Pinacate lava field (32°N, 113°30'W) to a low of +40 gammas north of the Copper Mountains (32°30'N, 113°55'W). A strong northwesterly trend characterizes the aeromagnetic map.

Reproduced with permission of the copyright owner. Further reproduction prohibited without permission.

Broadly speaking, the large amplitude, narrow magnetic anomalies (>100γ and <5 km across) occur over the schists and gneisses of the northern Gila Mountains and the cinder cones, flows, and dikes of the Pinacate lava field. Other large amplitude, broad magnetic anomalies (>150γ and ∿10 km across) occur over a large body of gneissic granite porphyry north and northeast of the Pinacate lava field. In the southwestern half of the map, all the anomalies have a small amplitude (<100γ) and are from 10 to 25 km across.

The difference in the breadth of magnetic anomalies is indeed striking and is important in that it indicates an extreme difference in depth to the magnetic rocks between the northeastern and southwestern portions of the aeromagnetic map. This difference in depth to anomaly source will be examined more carefully in a subsequent section.

Anomaly trends

The trend of magnetic anomalies over an area reflects to some degree the structural and lithologic trends of the various rock types within the area. For the geologic trends to be confidently determined from an aeromagnetic survey, they must be at least as long as the flight line separation. For this particular aeromagnetic survey, then, geologic trends should be more than five kilometers long to be confidently detected. However, once a magnetic trend is verified, it is not always possible to determine if it is due to trends in the lithology, the structure, or a combination of the two.

By slightly modifying a trend compilation technique discussed by Affleck (1963), I constructed the magnetic anomaly trend diagram of figure 19 for northwestern Sonora and southwestern Arizona. This

Reproduced with permission of the copyright owner. Further reproduction prohibited without permission.

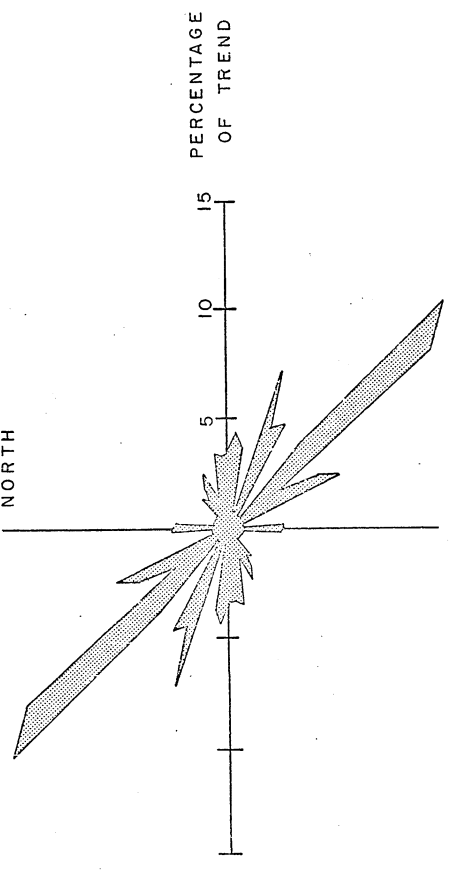

Figure 19. The azimuth and strength of primary magnetic anomaly trends (closed highs and lows) for northwestern Sonora and southwestern Arizona, plotted on 5° increments.

Reproduced with permission of the copyright owner. Further reproduction prohibited without permission.

diagram was made using primary magnetic trends (closed magnetic highs and lows) which extend across at least two flight lines. The azimuth and length of the lines drawn along the axes of the magnetic anomalies are compiled in 5° azimuth increments. The length of each trend line is divided by the total length of all the lines and multiplied by 100% so the trend along a particular azimuth may be expressed as a percentage of the total trend.

As can be seen from figure 19, over 30% of the magnetic anomaly trends lie between 310° and 320° (N40°W - N50°W). Additional trends are clustered between 60° and 100° (25%), 290° and 300° (∿17%), 330° and 335° (∿10%), and 355° and 5° (∿7%).

Lithologic units with distinctive magnetizations and elevation variations in the magnetic rocks are the primary source for the magnetic trends.

Some of the magnetic anomaly trends in the area are fairly easy to relate to either structural or lithologic trends while other magnetic trends have no obvious source. Faults having both strike-slip and normal components strike northwesterly through the area to form the elongate system of mountains and valleys as well as the structural framework for the Gulf of California -- Salton tectonic trough. These Cenozoic faults, which cause the elongate, northwesterly trending topography, can be equated with the strong magnetic anomaly trend between 310° and 320° as well as the anomaly trend between 330° and 335°. It may be that older lithologic or structural trends also influence the northwesterly magnetic trends since foliations and lineations of minerals in a presumed pre-Cambrian gneiss mapped by Gilluly (1946) in the Ajo area (see figure 20) show a preferred northwesterly trend. However,

Reproduced with permission of the copyright owner. Further reproduction prohibited without permission.

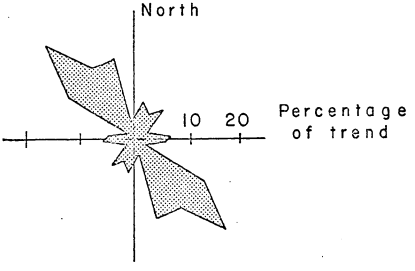

Figure 20. Mineral and lithologic trends in the Cardigan gneiss (Precambrian?) of the Ajo area (Gilluly, 1946) plotted in 10° azimuth increments. Trends determined from foliations with dips greater than 45°.

Reproduced with permission of the copyright owner. Further reproduction prohibited without permission.

these mineral trends may be localized and are on a small enough scale that they could not be detected by this regional aeromagnetic survey.

The magnetic trend lying between 60° and 100° can for the most part be related to the trends of, and contacts between, schists, gneisses, and granitic rocks of Mesozoic age and older. A large portion of these magnetic trends arise from an east-northeasterly trending body of porphyritic granitic gneiss north and east of the Sierra del Pinacate.

The magnetic anomaly trends which have azimuths between 290° and 300° are located primarily over areas covered by alluvium so that it is difficult to say what sort of geologic features cause them.

In summary, it is possible to relate many magnetic anomaly trends with broad lithologic and structural trends. Magnetic trends which cannot be directly correlated to some large-scale geologic feature may arise from older, less obvious lithologic trends in the crystalline basement or from effects of minor faulting.

Geologic model cross sections from aeromagnetic profiles

The elongate nature of the magnetic anomalies lends itself readily to two-dimensional modeling techniques. Figure 21 shows the location of profiles used to construct model geologic cross sections.

The gravity modeling for the preceding section determined the depth and configuration of the basement-sediment interface over the northeastern portion of the area. Results of seismic refraction surveys by Phillips (1964) in the northern Gulf were used to fix the depth to the basement-sediment interface in the southwestern part of the area which is about 5 km.

For a given magnetic profile over a known basement-sediment interface, any anomalies not due to the basement topography must be due to

Reproduced with permission of the copyright owner. Further reproduction prohibited without permission.

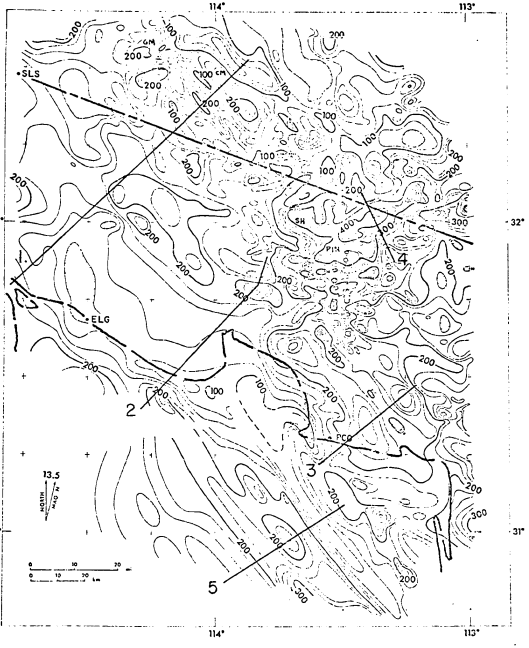

Figure 21. Location of profiles used to construct model geologic sections of Figures 22-25.

Reproduced with permission of the copyright owner. Further reproduction prohibited without permission.

magnetic changes in the rocks.

As a first-order modeling procedure, the boundaries and approximate magnetizations (see table 4) of bodies were found using a generalized slab of unit magnetization. A two-dimensional computer program described by Talwani and Hiertzler (1964) and adapted by Cady (pers. comm.) for the Stanford Fortran Five system was used to refine the first-order approximations. Figures 22,23,24, and 25 show the results of this modeling procedure for the profiles located in figure 21.

Reproduced with permission of the copyright owner. Further reproduction prohibited without permission.

TABLE 4

Rock Unit	Induced magnetization (in direction of present earth's field-0.5 oersted inducing field) ($\times 10^{-6}$ emu/cc)	Remanent magnetization (assumed parallel to present earth's field) ($\times 10^{-6}$ emu/cc)
granitic and gneissic rocks	20 - 260* avg. ~175	$\leq$175
Miocene(?) extrusives (rhyodacite)	0 - 490* avg. ~250	100 - 150
Pliocene(?) basalts	200 - 650*	~1000
Metamorphic rocks	20 - 1000* too few samples to give any average.	small
Pinacate basalt	600 - 1000* avg. ~800	2700 - 4000
Sediments (one sample)	22.3	small

*Range of samples measured.

TABLE 4. Induced and remanent magnetization for different major rock units.

Reproduced with permission of the copyright owner. Further reproduction prohibited without permission.

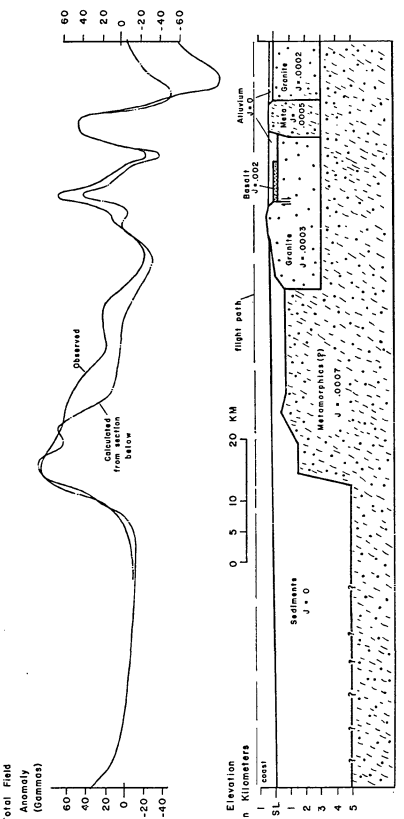

Figure 22. Total field profile and model geologic section for profile 1 of Figure 21.

Reproduced with permission of the copyright owner. Further reproduction prohibited without permission.

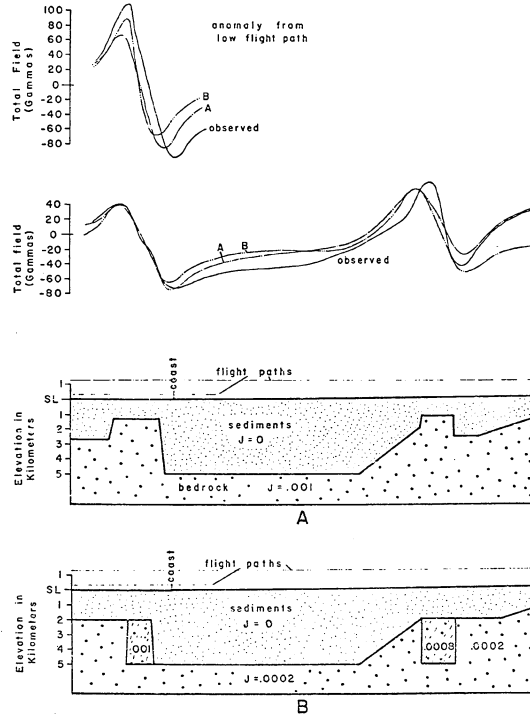

Figure 23. Total field profile and two model geologic sections for profile 2 of Figure 21. A) Constant magnetization of the crystalline basement assumed B) Changes in magnetization in crystalline basement assumed.

Reproduced with permission of the copyright owner. Further reproduction prohibited without permission.

Reproduced with permission of the copyright owner. Further reproduction prohibited without permission.

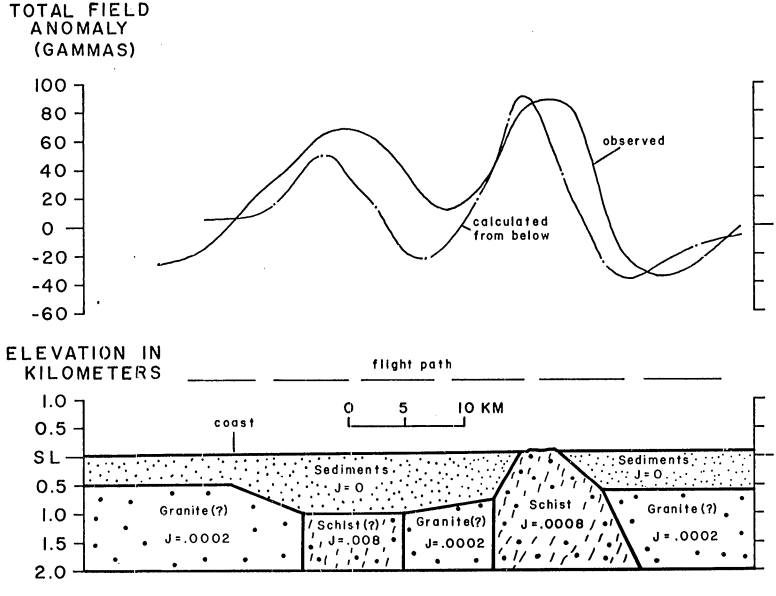

Figure 24. Total field profile and model geologic section for profile 3 of Figure 21.

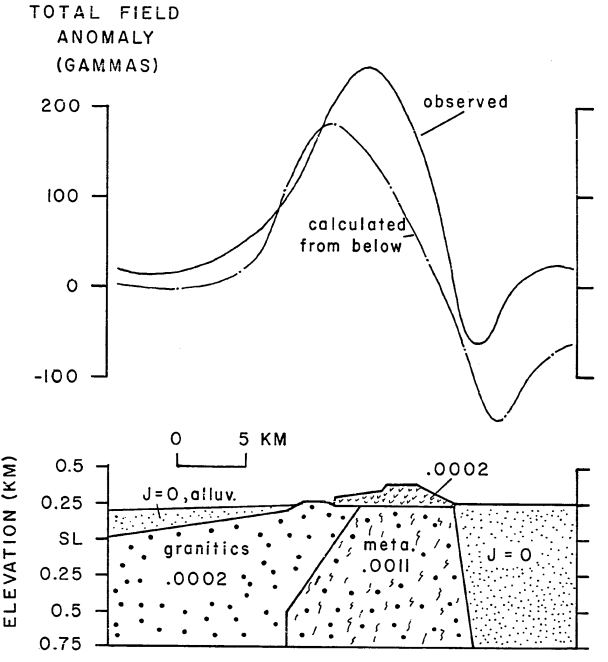

Figure 25. Total field profile and model geologic section for profile 4 of Figure 21. Small v's mark Pliocene(?) basalt. Magnitude and direction of remanence for the basalt used in modeling are shown in tables 3 and 4. Flight elevation is 1.3 kms; depth of bodies is 3 kms.

Reproduced with permission of the copyright owner. Further reproduction prohibited without permission.

IV. DISCUSSION

1. STRUCTURAL FEATURES

The structural control of the Pinacate lava field is not obvious because the lava field itself obscures any features present in the underlying crystalline rocks. From the gravity data, northwesterly trending basins and ranges extend beneath the Pinacate field. From the aeromagnetic map of figure 14 these northwesterly trending structures are interrupted by a cross cutting feature since there is a break in several of the northwesterly trending anomalies at the southwestern edge of the field. The break in these anomalies lies along a northeasterly trending line which extends from northeasterly aligned grabens west of the Bahia de Aduar (31°37', 114°7') across the Bahia de Aduar into the Sierra del Pinacate (31°51', 113°30'). So, from geophysical data, it can be said that the Pinacate lava field lies on the intersection between the northwesterly trending faults which form the elongate basins and ranges and an east-northeasterly (60°) cross-cutting structure. The 60° trend is probably a fault-controlled feature such as a graben, but there is not enough gravity data to the southwest of the lava field to make a more definite interpretation.

Another explanation for the presence of the Pinacate lava field has been proposed by Hey and Morgan (1971). They point out that stationary hot spots in the mantle have sufficient energy to provoke extensive vulcanism in the overlying crust. The Pinacate field is taken as the endpoint of a trend which extends through the San Juan seamount. This trend has formed as the Pacific and

Reproduced with permission of the copyright owner. Further reproduction prohibited without permission.

American plates move westerly over a stationary hot spot in the mantle. This is not a completely satisfactory explanation, for it does not explain the present lack of volcanic activity in the Pinacate area nor does it consider the influence that strike slip activity of the San Andreas fault system has had upon the Sierra del Pinacate.

The geologic cross-sections modeled in preceeding gravity and magnetic sections allow tectonic features such as the basin bounding faults to be located. Figure 26 shows the faults with dip-slip components in excess of 150 meters (3 mgals for a 0.5 gm/cc density contrast) which have been inferred from the gravity and aeromagnetic data. Figure 26 also shows the location under the alluvium of some of the magnetically distinctive units such as the gneissic granite porphyry, which is the most magnetic unit of the crystalline basement rocks, and the Pliocene(?) basalt.

To test the idea that the area adjacent to the San Andreas fault system and the Salton tectonic trough are themselves in zones of transform faulting and strike slip deformation, contacts between distinctive units in the crystalline basement were examined for possible strike slip offset.

From the geologic map of figure 5, the contacts between the granitic and metamorphic rocks in Arizona can be interpreted to show the amount of strike slip displacement on the basin-forming faults. The northernmost contact starts at 32°30', 114°20' and extends roughly east to 32°35', 113°40'. This contact strikes north of east in each of the three mountain ranges where it is exposed. The southernmost contact starts at 32°15', 114°5' and

Reproduced with permission of the copyright owner. Further reproduction prohibited without permission.

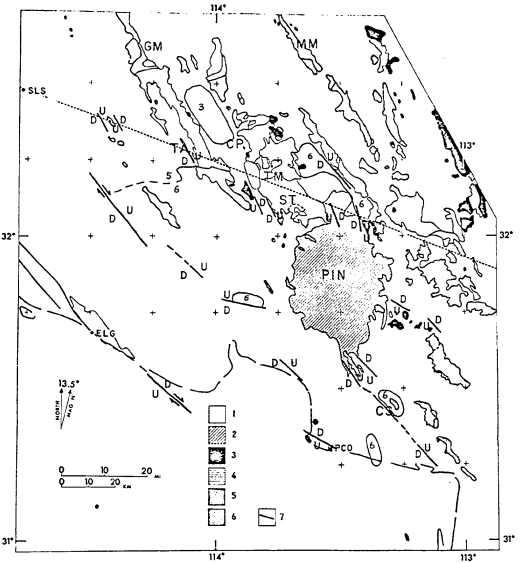

Figure 26. Structural and lithologic features located using geophysical techniques. Faults with vertical offset greater than 150 meters (3 mgals for a 0.5 gm/cc density contrast) are shown by heavy lines. Explanation of rock units and place name symbols is given in Figure 5.

Reproduced with permission of the copyright owner. Further reproduction prohibited without permission.

extends easterly to 32°15', 113°20'.

Figure 27 presents a simplified version of the strike-slip deformation in southwestern Arizona. From this figure, the total amount of strike-slip offset is about 20 km across the 50 km represented. The offset of the granite-metamorphic contact may not be a concrete enough measure of the amount of strike-slip deformation because the original contact may have been sinuous. The aeromagnetic data should be able to resolve this point by showing whether the contact is sharply offset on the basin bounding fault or has the offset taken up across the whole basin. However, the 5 kilometer flight line spacing could not resolve a sharp or gradual offset in the contact.

Other contacts did not extend from one range to the next and so could not be tested for possible strike slip offset. A cross check on the amount of strike-slip deformation comes from an analysis of the geometry of the vertical displacements on the faults. The expression found in the Geology Section relates strike-slip and normal offset on a fault. The relation is:

$$ss = \int_0^z \frac{z \, dz}{\tan\phi \, \tan\theta}$$

where ss = strike-slip offset, z = vertical offset, θ = dip of the fault plane, and ϕ = angle between fault trace and direction of small circle about pole of rotation for the plate boundary.

For the area of interest, the direction of the small circle is 315°. The faults in the Salton Trough trend at ∿317° while

Reproduced with permission of the copyright owner. Further reproduction prohibited without permission.

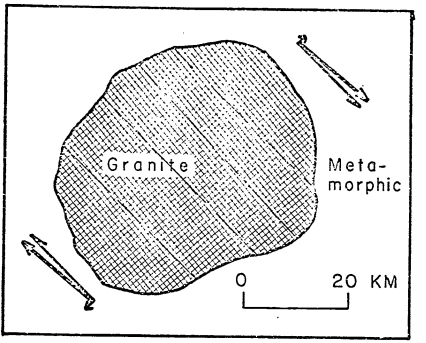

A

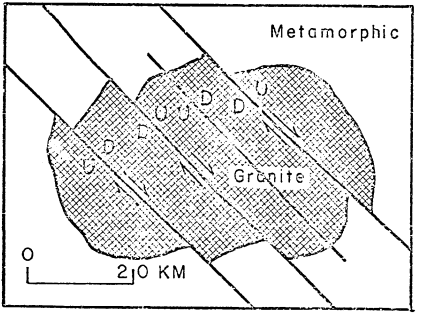

B

Figure 27. Simplified version of strike slip deformation in the crystalline basement. A) Original configuration of contact between granitic and metamorphic rocks. B) Configuration after strike slip deformation.

Reproduced with permission of the copyright owner. Further reproduction prohibited without permission.

those in Arizona trend from 320 to 330°. Additional gravity traverses would serve to better define the direction and amount of vertical offset on the basin-bounding faults. For a dip of 60°, the total amount of strike-slip offset across the Salton Trough and adjacent terrain in Arizona is

$$ss = \sum_{\ell=1,n} \frac{z_\ell}{\tan\phi_\ell \tan 60°}$$

For the faults listed in Table 5, the sum of strike-slip offsets in southwestern Arizona (20 km) agrees very well with that found from figure 27. The strike-slip offset across the Salton Trough (~100 km) is low when one considers a total expected offset of 240 km between the American and Pacific plates, but this may be due to several things. First, when ϕ is small, ss changes greatly for small changes in ϕ. Secondly, additional strike-slip offset must be taken up in adjacent terrain to the west as well as further to the east.

Reproduced with permission of the copyright owner. Further reproduction prohibited without permission.

TABLE 5

	Fault	z_ℓ (km)	ϕ_ℓ	Strike-slip Offset (km)
1)	Salton-west	5	2°2°	82
2)	Salton-east	5	6°	28
3)	Tinajas Altas-Mtns.	1.5	7°	7
4)	Cabeza Prieta Mtns.	1.5	9	7
5)	Mohawk Mtns.	1.5	12	6

TABLE 5. Strike-slip offset for major faults in the Salton Trough and southwestern Arizona.

Reproduced with permission of the copyright owner. Further reproduction prohibited without permission.

2. SUBDUED MAGNETIC ANOMALIES

The southwestern portion of the aeromagnetic map of Figure 14 contains broad, low amplitude anomalies (10-40 km, ~100γ). This zone of subdued anomalies contrasts sharply with the narrow, large amplitude anomalies (1-10 km, >100γ) of the rest of the aeromagnetic map. There are several possible explanations for this zone of subdued anomalies. The explanations can be divided into two broad groups. The first assumes that rocks of the crystalline basement exposed to the northeast also extend under the area of subdued anomalies. The second assumes that the crystalline basement under the area of subdued anomalies is lithologically different from rocks exposed to the northeast, being crust transitional between oceanic and continental.

From seismic refraction surveys by Kovach and others (1962) to the northwest and Phillips (1964) in the northern Gulf, the depth to crystalline basement is interpreted to be four to six kilometers in the northern Gulf.

Since the overlying sediments are essentially non-magnetic ($J_i < 20 \times 10^{-6}$ emu/cc; $J_r < 46 \times 10^{-6}$ emu/cc; Griscom and Muffler, 1971), any magnetic anomalies must have their source in the crystalline basement rocks or in bodies which may have intruded the thick sedimentary sequence. Extrusive bodies can be ruled out as a source of anomalies since they would cause large amplitude, narrow magnetic anomalies -- and none occur within the region of subdued anomalies.

From table 4, it is clear that there are large enough contrasts in the magnetizations of the crystalline basement rocks exposed

Reproduced with permission of the copyright owner. Further reproduction prohibited without permission.

to the northeast to explain the amplitude of anomalies in the magnetic smooth zone. The subdued magnetic anomalies could be due simply to the great depth to the crystalline basement. If one considers the high heat flow and thick insulating blanket of sediments, it is clear that there is also a shallow depth to the Curie isotherm (550°C), which serves only to broaden and subdue the anomalies more.

The depth to the Curie isotherm was determined in the following way: First, a heat flow of 3.0 microcal/cm^2/sec (Von Herzen, 1963) arising from sources deeper than the Curie isotherm was assumed. Second, from table 6, a conductivity of 5 x 10^{-3} cal/°C-cm-sec was assumed for the sediments and 8 x 10^{-3} cal/°C-cm-sec for the crystalline basement rocks. Assuming steady state conditions, the thermal gradient = heat flow/conductivity, so for sediments

$$T = \frac{3 \times 10^{-6}\ \text{HFU}}{5 \times 10^{-3}\ \text{cal/°C-cm-sec}} \cdot 10^{+5}\ \text{cm/km} = 60°\text{C/km}$$

and for crystalline rocks

$$T = \frac{3 \times 10^{-6}}{8 \times 10^{-3}\ \text{cal/°C-cm-sec}} \cdot 10^{+5}\ \text{cm/km} = 37°\text{C/km}$$

For 5 km of sediments, the depth to the Curie isotherm (550°C) is about 11 km.

In addition to a shallow Curie depth, a broad gravity high over the northern Gulf indicates that there is a general thinning of the crust in the area. This means that the crust in the northern Gulf may be pervasively intruded by basaltic magma and thus may be a

Reproduced with permission of the copyright owner. Further reproduction prohibited without permission.

TABLE 6

ROCK TYPE	CONDUCTIVITIES (CAL/°C-CM-SEC)
Granite-Gneiss (1)	$7 - 8 \times 10^{-3}$
Volcanics (1)	$5 - 7 \times 10^{-3}$
Seds in Salton Sea Geothermal Field (2)	3.5×10^{-3}
Seds. in Wilson #1 Well (2)	5×10^{-3}
Oceanic Seds. (ooze, red clay) (1)	2×10^{-3}
Water (1)	1.5×10^{-3}

(1) Clark, 1966

(2) Muffler and White, 1969

Table 6. Thermal conductivities of selected earth materials.

Reproduced with permission of the copyright owner. Further reproduction prohibited without permission.

crust which is transitional between oceanic and continental. However, the magnetic data will not be able to resolve whether the crust in the northern Gulf is continental or transitional because there is not a distinctive contrast in magnetization between the two cases. In a simple example, if an original continental crust with a magnetization of 200 x 10^{-6} emu/cc is intruded by basaltic dikes, with magnetizations of 1400 x 10^{-6} emu/cc, which after intrusion account for one third of the crust, then the apparent magnetization contrast would be about 600 x 10^{-6} emu/cc, -- exactly as assumed for a continental crust. Consequently, the model cross sections of figure 28 can represent either a continental or a transitional crust.

Figure 28 shows two possible model cross sections. The magnetizations are taken parallel to the direction of the present earth's field. The two different model configurations of figure 29 adequately fit the constraints imposed by gravity data (Harrison and Mathur, 1964) and seismic data (Phillips, 1964) in the northern Gulf. The model cross section of figure 28a assumes that magnetization contrasts in the basement rocks cause the magnetic anomalies. The model cross section of figure 28b assumes a constant magnetization of 1000 x 10^{-6} emu/cc for a crystalline basement which has enough topographic relief to account for the observed total field magnetic anomalies.

In summary, the subdued magnetic anomalies are due to moderately magnetic continental or transitional crustal rocks buried beneath 5 kilometers of sediments and with a shallow Curie isotherm.

Reproduced with permission of the copyright owner. Further reproduction prohibited without permission.

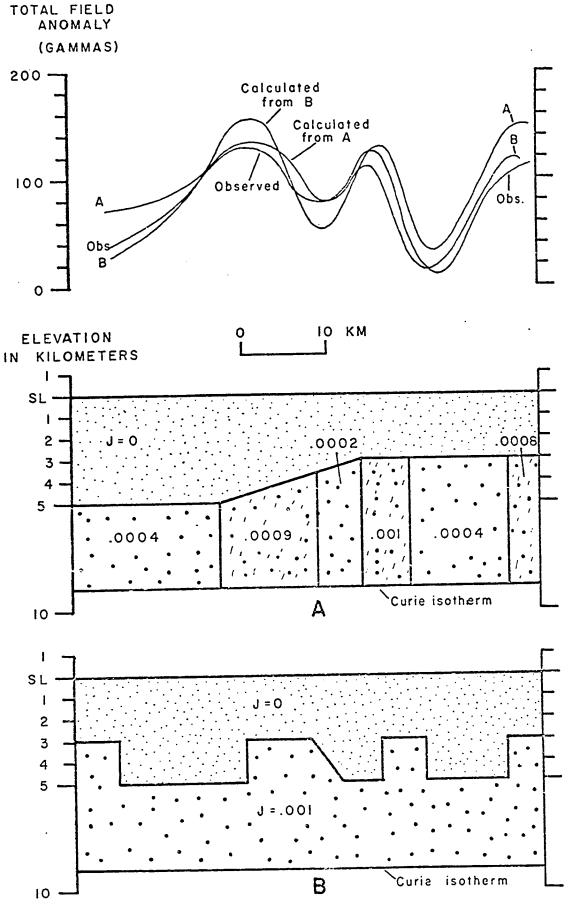

Figure 28. Total field profile and model geologic sections over zone of subdued magnetic anomalies in the northern Gulf of California. (Profile 5 of Figure 21). A) Constant depth to crystalline basement assumed; changes in magnetizations cause anomalies B) Constant magnetization of the basement rocks assumed.

Reproduced with permission of the copyright owner. Further reproduction prohibited without permission.

If the subdued magnetic anomalies are due to some sort of transitional crust, for instance one which is heavily injected by basaltic dikes, then the anomalies should lie over the zone of extensional deformation, where basaltic magma would be easily intruded along extensional cracks. As can be seen from the aeromagnetic map of figure 14, the magnetic anomalies over the northern Gulf do not trend northeasterly as they would if basalt were being injected in a portion of the crust undergoing extension, but on the contrary, trend northwesterly. The northwesterly trend indicates that either injection is occurring along the strike-slip faults of the San Jacinto fault system or else that large crustal blocks of differeing magnetizations have become juxtaposed. Such a juxtapositioning of crustal blocks could arise from movement on strike-slip faults or could represent the original configuration of rock units in the crust.

The area of subdued magnetic anomalies at the head of the Gulf of California presents an opportunity for comparison with other magnetically smooth zones in the Red Sea, Gulf of Aden, and the North Atlantic. A review of suggestions regarding these magnetic smooth zones has been made by Emery and others (1970), and the specific ideas to follow have been discussed to some degree by Irving (1970) and Vogt and others (1970).

Zones of subdued magnetic anomalies occur along the margins of the North Atlantic, the Red Sea and Gulf of Aden, and over the basins in the northern Gulf of California. These zones of subdued ($<100\gamma$) magnetic anomalies are in sharp contrast to the large amplitude ($250-1000\gamma$) magnetic anomalies which occur over the deep oceans

Reproduced with permission of the copyright owner. Further reproduction prohibited without permission.

as well as the short wave length, high amplitude anomalies found over the continents. As noted by Irving (1970), these smooth zones have three notable features: they occur around the margins of spreading centers, they have different ages, and their boundaries are not isochronous. Thus, the smooth zones must have a geologic origin (Irving, 1970) related to the initial tectonic activity during the formation of the spreading center.

Figure 29 shows the location of regions having subdued and large amplitude magnetic anomalies in the Red Sea, Gulf of Aden, and Gulf of California. A comparison of the magnetic profiles located in figure 29 is shown in figure 30. The smooth zones in these areas are from 150 to 400 kilometers wide.

If the interpretation made in this section for the subdued anomalies in the northern Gulf of California is valid -- namely that the anomaly sources under the smooth zones are deeply buried continental or transitional crustal rocks, then this interpretation should apply to other areas with subdued anomalies.

It is here concluded that the regions of subdued magnetic anomalies develop during the original formation of a spreading center. The original rift forms a broad, deep central graben which fills with sediments. Initially there might be little or no vulcanism associated with the newly-formed rift. Heat flow over the region would be high due to increased magmatic activity, and consequently the depth to the Curie isotherm would be shallower than in adjacent crust. The combination of a deep rift and shallow Curie isotherm would lead directly to a zone of subdued magnetic anomalies. This example would be directly applicable to subdued anomalies in

Reproduced with permission of the copyright owner. Further reproduction prohibited without permission.

Reproduced with permission of the copyright owner. Further reproduction prohibited without permission.

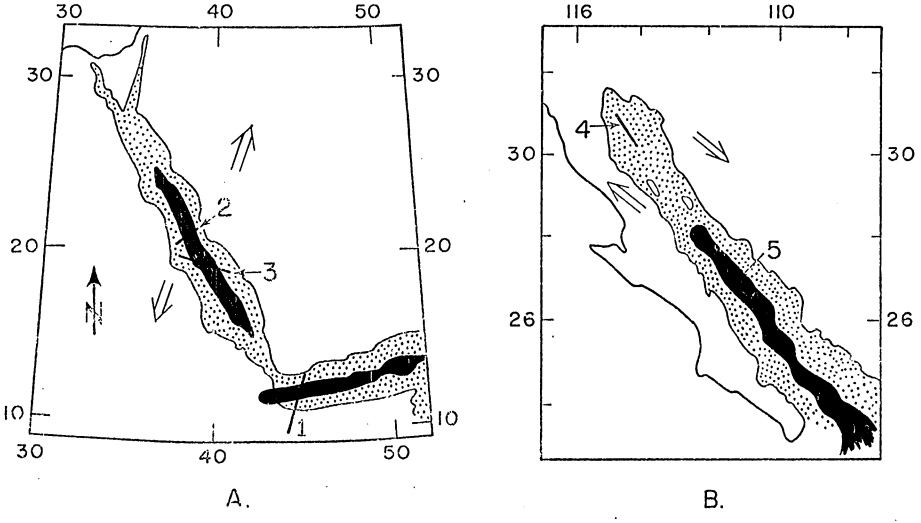

Figure 29. Regions of subdued (stippled) and large amplitude (red) magnetic anomalies in A) Red Sea and Gulf of Aden, B) Gulf of California.

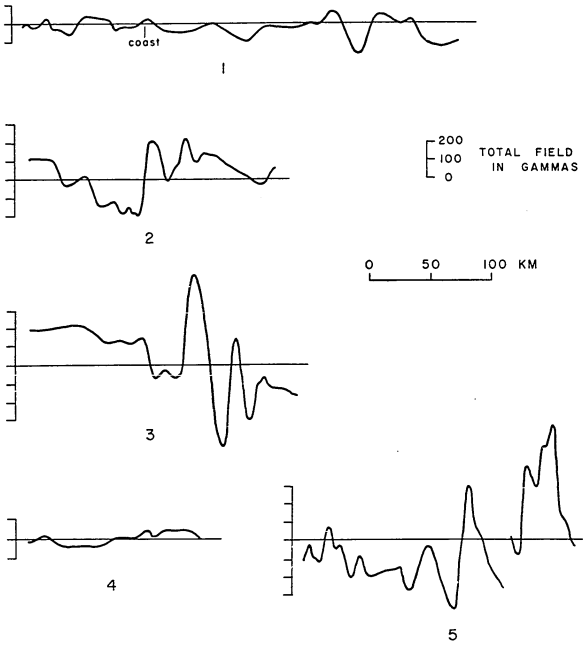

Figure 30. Magnetic profiles of Figure 29 showing subdued and large amplitude anomalies in the Red Sea, Gulf of Aden, and Gulf of California.

Reproduced with permission of the copyright owner. Further reproduction prohibited without permission.

the northern Gulf of California, which has anomalies even more subdued than those in the Red Sea.

Even with igneous activity in a newly formed rift, as suggested by Vogt and others (1970), little basaltic magma would reach the surface through the blanket of low density sediments, but would form dikes and sills at depth. The slow cooling rate of these basaltic intrusives would prevent formation of large magnetic remanence and consequently there would be no large anomalies associated with the volcanic activity. This is certainly the situation for the Salton Trough where Griscom and Muffler (1971) report a large basaltic intrusive body at depth under the Salton Sea. Except for local anomalies over rhyolite domes, this body has only a broad, low amplitude (40 km, 200γ) anomaly over it.

With continued spreading, the rift becomes broad enough so that a smaller rate of sedimentation occurs near the central portion of the rift, which is now farther removed from sediment sources in the adjacent continental blocks, allowing easy extrusion of basalt and subsequent formation of large magnetic anomalies. Figure 31 illustrates this parallel sequence of spreading and formation of magnetic anomalies.

Reproduced with permission of the copyright owner. Further reproduction prohibited without permission.

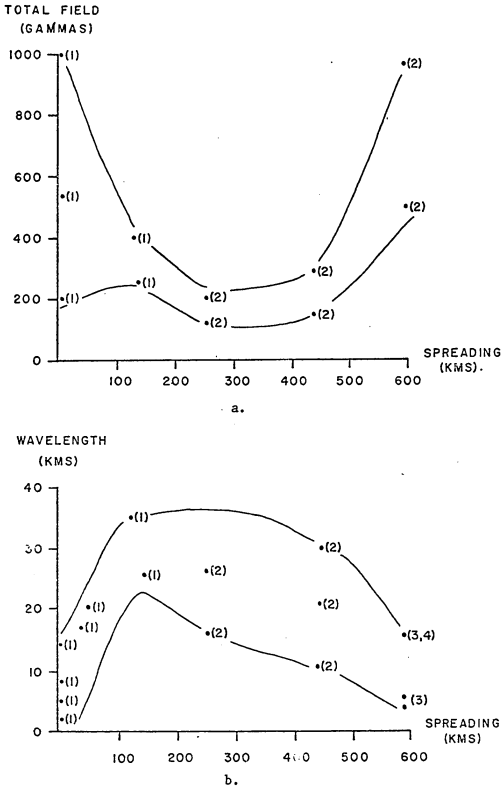

Figure 31. Relationship between amount of spreading and magnetic anomalies through the transitional region between continental crust (0 km spreading) and oceanic crust (>500 km spreading). a) Amplitude of anomalies (maximum values). b) Wavelength of anomalies (minimum values). Source of data: 1 - Taylor and others, 1968; 2 - Vogt and others, 1970; 3 - Larson and Speiss, 1968; 4 - Moore and Buffington, 1968.

Reproduced with permission of the copyright owner. Further reproduction prohibited without permission.

V. CONCLUSIONS

Northwesterly trending strike-slip faults in the area are the result of deformation associated with movement between two large plates of the earth's crust. Movements on these strike-slip faults offset and juxtapose differing lithologies and cause vertical offset across the faults; as a result, the predominant trend of gravity and magnetic anomalies in the area is northwesterly.

Gravity measurements indicate that basin sediments northwest, north, and east of the Pinacate lava field are from 250 to 650 meters thick. South of the lava field and north of Puerto Peñasco, Sonora, basin sediments are about 1500 meters thick.

Results of previous seismic refraction work (Phillips, 1964) indicate that there are about 5 kilometers of sediments in the northern Gulf. The gravity measurements do not reflect this deep sedimentary trough for two reasons. First, the siltstones and sandstones increase in density with depth so that the density contrast in the lower part of the section is very small. Second, there is a general thinning of the crust from the area to the northeast across the northern Gulf and Salton trough. This causes a broad gravity high which tends to mask the gravity low associated with sediments in the Salton and Gulf tectonic troughs.

The metamorphic rocks, particularly a gneissic granite porphyry, are about three times as magnetic as the biotite granites. The more mafic metamorphic rocks are primarily biotite schist with magnetizations which range from those of the granites to

Reproduced with permission of the copyright owner. Further reproduction prohibited without permission.

those of the gneissic granite porphyry. The extrusive rocks have remanent magnetizations two to six times as great as induced magnetizations (at 0.5-oersted inducing field). The basaltic extrusives are about four times as magnetic as the biotite granites while the more felsic extrusives have magnetizations comparable to the granites.

Model geologic cross sections constructed using the observed rock magnetizations to fit observed magnetic profiles show that several of the basins in the northern part of the area (in Arizona) contain extensive buried sheets of basalt. Model cross sections also show a drastic increase in depth to the crystalline basement (to five kilometers) in the southwestern part of the area.

The Pinacate volcanic field lies on the intersection of an east northeasterly magnetic cross trend with the northwesterly trending faults which form the basins and ranges. The cross trend extends from small grabens near the coast of the Gulf of California into the Sierra del Pinacate.

Subdued magnetic anomalies in the northern Gulf, which extend northwesterly to the Salton Trough, are interpreted as due to deeply buried crust which has a shallow Curie isotherm. It is not possible from the aeromagnetic data to discern a continental crust, such as that exposed to the northeast, from a crust transitional to oceanic. An extension of this interpretation to other magnetically smooth zones in the Red Sea and North Atlantic suggests that the magnetic smooth zones are an inherent feature of an incipient spreading center.

Reproduced with permission of the copyright owner. Further reproduction prohibited without permission.

The various tectonic features of the region at the head of the Gulf of California indicate that tectonic activity in the area is the result of interaction between two large plates of the earth's crust as they move by one another. The subdued magnetic anomalies, the earthquake swarms, the volcanism in the northern Gulf and Salton Trough, and the depth of the Salton Trough are all indicators of incipient spreading centers. The strike-slip faults, both within and adjacent to the Salton Trough, and the ranges which lie approximately parallel to the direction of strike-slip deformation are indicators of transform faulting. Strike-slip faults make a small angle with the small circle about the pole of relative motion between the two plates. As a consequence, spreading occurs on the strike-slip faults as well as at centers of spreading.

Reproduced with permission of the copyright owner. Further reproduction prohibited without permission.

BIBLIOGRAPHY

Affleck, J., Magnetic anomaly trend and spacing patterns, Geophys. 28 (3), 379-395, 1963

Allison, E. C. Geology of areas bordering Gulf of California in van Andel, T. H., and Shor, G. G., Jr., eds., Marine geology in the Gulf of California, Amer. Assoc. Petroleum Geol., Mem. 3, 3-29, 1964

Alonzo-Espinoza, H., and Mooser, F., El pozo M-3 del campo geotermico del Cerro Prieto, B. C. México, Assoc. Mexicana de Geologos Petroleros Bol., 16(7-8), 163-178, 1964

Atwater, Tanya, Implications of plate tectonics for the Cenozoic tectonic evolution of western North America, Geol. Soc. Amer., Bull. 81, 3513-3536, 1970

Beal, C. H., Reconnaissance of the geology and oil possibilities of Baja California, Mexico, Geol. Soc. Amer. Mem. 31, 1948

Bhuyan, Ganish, Gravity base stations in Arizona, Master's Thesis, University of Arizona, Tucson, 1965

Biehler, Shawn, Gravity models of the crustal structure of the Salton Trough, Geol. Soc. Amer.,Cord. Sec.,67th Ann. Mtg., 3(2), 82-83, 1971

Biehler, S., Kovach, R. L., and Allen, C. R., Geophysical framework of northern end of Gulf of California structural province, in van Andel, T. H., and Shor, G. G. Jr., eds., Marine Geology in the Gulf of California, Amer. Assoc. Petr. Geol. Mem. 3, 126-143, 1964

Bryan, Kirk, Erosion and sedimentation in the Papago country, Arizona--with a sketch of the geology, U. S. Geol. Surv. Bull. 730B, 19-90, 1923

Bryan, Kirk, The Papago country, Arizona; a geographic, geologic, and hydrologic reconnaissance with a guide to desert watering places, U. S. Geol. Surv. Water-Supply Ppr. 498, 1925

Cain, J. C., and Cain, S. J., Derivation of the International Geomagnetic Reference Field, Report to IAGA Comm. II, Group 4 in J. Geomag. and Geoelec., 21(2), 569, 1969

Clark, S. P., Jr., Thermal conductivity in Clark, S. P., Jr., ed., Handbook of Physical Constants - Revised edition, The Geol. Soc. Amer. Mem. 97, 459-482, 1966

Damon, P. E., Mauger, R. L., and Sikerman, M., K-Ar dating of Laramide plutons and volcanic rocks within the Basin-Range province of Arizona and Sonora, in Int'l Geol. Cong. Rept. of the twenty-second sess., India, Part III, India Int'l Geol. Cong. Organizing Comm., Calcutta, India, 45-55, 1964

Reproduced with permission of the copyright owner. Further reproduction prohibited without permission.

Dibblee, T. W., Geology of the Imperial Valley region, California, in Jahns, R., ed., Geology of Southern California, Calif. Div. Mines and Geol. Bull., 170, 21-28, 1954

Emery, K. O., Uchupi, E., Phillips, J. D., Bowin, C. O., Bunce, E. T., and Knott, S. T., Continental rise of eastern North America, Amer. Assoc. Petroleum Geol. Bull., 54, 44-108, 1970

Fries, Carl, Jr., Resena de la geología del Estado de Sonora con enfasis en el Paleozoico, Asoc. Mex. de Geol. Petr., 14(11-12) 257-273, 1962

Gilluly, J. W., The Ajo Mining District, Arizona, U. S. Geol. Surv. Prof. Ppr. 209, 112, 1946

Girdler, R. W., The Red Sea - a geophysical investigation, in Degens, E. T., and Ross, D. A., eds., Hot brines and recent heavy metal deposits in the Red Sea, Springer-Verlag, N.Y., 38-58, 1969

Girdler, R. W., An aeromagnetic survey of the junction of the Red Sea, Gulf of Aden, and Ethiopian rifts--a preliminary report, Phil. Trans. Roy. Soc. Lon. Ser. A., 267, 359-368, 1970

Griscom, A. and Muffer, L. J. P., Aeromagnetic survey of the Salton Sea geothermal field, southeastern California, Geol. Soc. Amer., Cord. Sec., 67th Ann. Mtg., 3(2), 129, 1971

Harrison, J. C., and Mathur, S. P., Gravity anomalies in Gulf of California in van Andel, Tj. H., and Shor, G. G., Jr., eds., Marine geology in the Gulf of California, Amer. Assoc. Petroleum Geol., Mem. 3, 76-89, 1964

Hawkins, J. W., Petrology and possible tectonic significance of late Cenozoic volcanic rocks, Southern California and Baja California, Geol. Soc. Amer., Bull., 81, 3323-3338, 1970

Hey, R. N., and Morgan, W. J., Parallel seamount chains in the northeast Pacific, Trans. Amer. Geophys. Union, 52(4), 236, 1971

Irving, E., The Mid-Atlantic Ridge at 45°N. XIV. Oxidation and magnetic properties of basalt, a review and discussion, Canadian Journ. Earth Sci., 7, 1528-1538, 1970

Jahns, R. H., Collapse depressions of the Pinacate volcanic field, Sonora, Mexico, in Arizona Geological Society Guidebook 2, Ariz. Geol. Soc. Digest, 2nd Ann., 165-183, 1959

King, P. B., Tectonic map of North America, Denver, Colo., U. S. Geol. Surv., 2 sheets, 1969

Kovach, R. L., Allen, C. R., and Press, F., Geophysical investigations in the Colorado Delta region, J. Geophys. Res., 67(7), 2845-2871, 1962

Reproduced with permission of the copyright owner. Further reproduction prohibited without permission.

Larson, P. A., Mudie, J. D., Hilde, T. W. C., and Larson, R. L., Sea-floor spreading in the Gulf of California?, Trans. Amer. Geophys. Union, 51(4), 330, 1970

Larson, R. L., Menard, H. W., and Smith, S. M., Gulf of California, a result of ocean-floor spreading and transform faulting, Science, 161, 781-784, 1968

Larson, R. L., and Speiss, F. N., East Pacific Rise crest, a near bottom geophysical profile, Science, 163, 68-71, 1969

Lipman, P. W., Prostka, H. J., and Christensen, R. L., Cenozoic volcanism and tectonism in the western United States and adjacent parts of the spreading ocean floor. Part 1, early and middle Tertiary, Geol. Soc. Amer., Cord. Sec., 66th Ann. Mtg., 2(2), 112, 1970

Lord, E. C., Petrographic report on rocks from the United States-Mexico boundary, U. S. Nat'l Museum Proc., 21(1173), 773-781, 1899

McKenzie, D. P., and Morgan, W. J., The evolution of triple junctions, Nature, 224, 125-133, 1968

Mercado, S., Cerro Prieto geothermal field, Baja California, Mexico, Trans. Amer. Geophys. Union, 50(2), 59, 1969

Moore, D. G. and Buffington, E. C., Transform faulting and growth of the Gulf of California since late Pliocene, Science, 161, 1230-1241, 1968

Morgan, W. J., Rises, trenches, great faults, and crustal blocks, J. Geophys. Res., 73, 1959-1982, 1968

Muffler, L. J. P., and White, D. E., Active metamorphism of Upper Cenozoic sediments in the Salton Sea geothermal field and the Salton Trough, southeastern California, Geol. Soc. Amer., Bull., 80, 157-182, 1969

National Oceanic and Atmospheric Administration, Preliminary determination of epicenters, Monthly listing, U. S. Dept. of Commerce, Rockville, Md., 1969-1971

Phillips, R. P., Seismic refraction studies in the Gulf of California in van Andel, T. H., and Shor, G. G., Jr., eds., Marine geology in the Gulf of California, Amer. Assoc. Petroleum Geol., Mem. 3, 90-121, 1964

Rusnak, G. A., Fisher, R. L., and Shepard, F. P., Bathymetry and faults of Gulf of California in van Andel, T. H., and Shor. G. G., Jr., eds. Marine geology of the Gulf of California, Amer. Assoc. of Petroleum Geol., Mem. 3, 59-75, 1964

Reproduced with permission of the copyright owner. Further reproduction prohibited without permission.

Sumner, J. R., Tectonic significance of gravity and aeromagnetic investigations in Sonora and Arizona at the head of the Gulf of California, Geol. Soc. Amer., Cord. Sec., 67th Ann. Mtg., 3(2), 204, 1971

Sykes, L. R., Mechanism of earthquakes and nature of faulting on the mid-oceanic ridges, J. Geophys. Res., 72(8), 2131-2153, 1967

Sykes, L. R., Earthquake swarms and sea-floor spreading, J. Geophys. Res., 75(32), 6598-6611, 1970

Talwani, M., and Hiertzler, J. R., Computation of magnetic anomalies caused by two dimensional structures of arbitrary shape, in Parks, G. A., ed., Computers in the mineral industries-Part I, Stanford University Publ. Geol. Sci., 9(1), 46/-480, 1964

Talwani, M., Worzel, J. L., and Landisman, M., Rapid gravity computations for two-dimensional bodies with application to the Mendocino submarine fracture zone, J. Geophys. Res., 64, 49-59 1959

Taylor, P. T., Zietz, I., and Dennis, L. S., Geologic implications of aeromagnetic data for the eastern continental margin of the United States, Geophys., 33(5), 755-780, 1968

Thatcher, W., An oceanic ridge earthquake swarm, northern Gulf of California, March, 1969, Trans. Amer. Geophys. Union, 51(4), 357, 1970

Thatcher, W. and Brune, J. N., Seismic study of an oceanic ridge earthquake swarm in the Gulf of California, Bull. Seism. Soc. Amer., 61, in press

Thompson, G. A. and Sandberg, C. H., Structural significance of gravity surveys in the Virginia City-Mount Rose area, Nevada and California, Geol. Soc. Amer. Bull., 69, 1269-1282, 1958

United Nations Development Programme, Survey of metallic mineral deposits in Mexico (DP/SF/UN/-19-Mexico) United Nations, N.Y., 1969

Vine, F. J., Spreading of the ocean floor - new evidence, Science, 154, 1405-1415, 1966

Vogt, P. R., Anderson, C. N., Bracey, D. R., and Schneider, E. D., North Atlantic magnetic smooth zone, J. Geophys. Res., 75, 3955-3968, 1970

Von Herzen, R. P., Geothermal heat flow in the Gulfs of California and Aden, Science, 140(3572), 1207-1208, 1963

Wilson, E. D., Geology and mineral deposits of southern Yuma County, Arizona, Ariz. Bureau Mines, Bull. 134, 234, 1933

Reproduced with permission of the copyright owner. Further reproduction prohibited without permission.

Wilson, I. F., Buried topography, initial structures, and sedimentation in Santa Rosalia area, Baja California, Mexico: Amer. Assoc. Petroleum Geol. Bull., 32, 1762-1807, 1948

Woollard, G. P., and Rose, J. C., International Gravity Measurements, Soc. Exploration Geophys., George Banta Co., Menasha, Wisc., 1963

Reproduced with permission of the copyright owner. Further reproduction prohibited without permission.

APPENDIX A

Gravity Stations

STATION	LATITUDE (DEG,MIN)	LONGITUDE (DEG,MIN)	ELEV. (FT)	OBS. GRAV. (MGAL)	B.A. (MGAL)
CCCO	31 58.65	113 21.75	0660.0	979417.63	-37.20
0001	31 58.66	113 21.30	0654.0	979419.00	-36.80
0002	31 57.76	113 21.30	0651.0	979420.66	-34.20
0003	31 56.74	113 21.30	0647.0	979417.97	-35.60
0004	31 48.80	113 17.70	0555.0	979410.46	-37.40
8888	31 50.95	113 22.40	0811.0	979397.53	-38.94
0005	31 49.60	113 18.10	0560.0	979412.13	-37.10
0006	31 50.00	113 18.40	0555.0	979412.79	-37.20
0007	31 50.54	113 19.90	0570.0	979413.14	-36.70
0008	31 50.55	113 19.45	0570.0	979413.02	-36.90
0009	31 51.09	113 10.85	0615.0	979411.32	-36.60
0010	31 51.90	113 19.85	0630.0	979410.5	-37.20
0011	31 52.78	113 20.05	0665.0	979410.05	-37.00
0012	31 53.59	113 20.70	0690.0	979408.76	-38.00
0013	31 54.35	113 21.40	0715.0	979406.65	-39.60
0014	31 54.36	113 21.80	0749.0	979406.42	-37.80
0015	31 54.79	113 21.65	0680.0	979411.67	-37.30
0016	31 55.35	113 21.90	0640.0	979412.31	-39.80
0017	31 56.17	113 21.80	0635.0	979414.56	-39.00
0018	31 59.46	113 21.30	0660.0	979421.39	-35.10
0019	32 00.00	113 21.30	0655.0	979422.65	-34.80
0020	32 00.37	113 22.20	0670.0	979419.66	-37.40
0021	32 00.89	113 22.90	0710.0	979418.42	-37.00
0022	32 01.22	113 23.80	0720.0	979416.05	-39.30
0023	32 01.49	113 24.70	0688.0	979413.58	-44.00
0024	32 01.85	113 25.80	0926.0	979407.99	-47.80
0025	32 02.25	113 26.80	0728.0	979403.76	-52.50
0026	32 02.48	113 27.70	0763.0	979401.38	-53.00
0027	32 02.75	113 28.80	0731.0	979407.61	-52.10
0028	32 02.72	113 29.90	0764.0	979407.95	-46.70
0029	32 02.50	113 31.10	0758.0	979412.50	-42.20
0030	32 02.61	113 32.20	0743.0	979415.44	-40.30
0031	32 02.82	113 32.20	0735.0	979413.57	-43.30
0032	32 03.29	113 34.60	0721.0	979413.59	-44.50
0033	32 03.32	113 35.70	0726.0	979413.61	-44.20
0034	32 03.36	113 37.00	0765.0	979413.64	-41.90
0035	32 04.07	113 39.80	0806.0	979409.56	-44.40
0036	31 50.85	113 22.60	0832.0	979395.02	-39.60
0037	31 50.81	113 21.60	0735.0	979403.21	-37.60
0038	31 50.72	113 21.00	0705.0	979405.28	-36.70
0039	31 50.46	113 20.80	0659.0	979407.47	-36.90
0040	31 50.16	113 20.40	0600.0	979410.07	-37.40
0041	31 49.92	113 19.90	0603.0	979411.45	-35.60
0042	31 49.86	113 19.40	0587.0	979413.18	-34.80
0043	31 49.52	113 19.00	0576.0	979412.78	-35.40
0044	31 40.75	113 18.60	0430.0	979418.78	-27.30
0045	31 40.08	113 19.10	0400.0	979419.04	-27.00
0046	31 39.26	113 19.60	0375.0	979419.89	-26.60

Reproduced with permission of the copyright owner. Further reproduction prohibited without permission.

STATION	LATITUDE (DEG,MIN)	LONGITUDE (DEG,MIN)	ELEV. (FT)	OBS. GRAV. (MGAL)	B.A. (MGAL)
0047	31 38.40	113 20.10	0355.0	979422.27	-24.60
0048	31 37.60	113 20.60	0335.0	979420.20	-26.40
0049	31 37.80	113 21.20	0320.0	979420.40	-27.40
0050	31 36.05	113 21.70	0300.0	979422.56	-24.00
0051	31 35.46	113 22.10	0280.0	979426.96	-19.90
0052	31 34.56	113 22.60	0265.0	979426.28	-20.50
0053	31 33.30	113 23.10	0244.0	979427.02	-20.00
0054	31 32.95	113 23.60	0234.0	979430.31	-16.80
0055	31 32.24	113 24.00	0209.0	979433.79	-13.20
0056	31 31.41	113 24.60	0192.0	979427.00	-19.80
0057	31 31.88	113 24.30	0180.0	979430.47	-17.80
0058	31 30.55	113 25.20	0170.0	979419.81	-27.30
0059	31 29.70	113 25.60	0170.0	979415.11	-30.80
0060	31 28.61	113 26.20	0150.0	979413.55	-32.10
0061	31 27.30	113 27.20	0136.0	979412.69	-32.40
0062	31 24.58	113 28.90	0120.0	979405.63	-36.50
0063	31 33.70	113 29.30	0065.0	979405.75	-38.17
0064	31 20.70	113 31.20	0049.0	979401.05	-40.10
0065	31 19.52	113 31.95	0039.0	979406.33	-33.80
0066	31 20.00	113 31.70	0045.0	979403.95	-36.40
0067	31 41.11	113 18.70	0410.0	979420.18	-26.60
0068	31 41.54	113 18.60	0415.0	979420.77	-26.30
0069	31 41.98	113 18.60	0420.0	979421.43	-25.90
0070	31 42.43	113 18.70	0435.0	979421.95	-25.20
0071	31 42.85	113 18.40	0444.0	979420.35	-26.25
0072	31 43.85	113 18.30	0455.0	979419.13	-28.70
0073	31 47.93	113 17.70	0550.5	979408.12	-39.40
0074	31 47.65	113 17.70	0543.0	979408.45	-39.20
0075	31 46.60	113 17.80	0522.0	979410.70	-36.80
0076	31 45.80	113 18.20	0500.0	979415.18	-32.50
0077	31 44.96	113 18.40	0485.0	979417.55	-30.00
0078	31 44.40	113 18.50	0470.0	979418.01	-29.60
0079	31 17.86	113 33.00	0020.0	979419.92	-19.20
0080	31 20.25	113 32.80	0036.0	979409.36	-31.90
0081	31 20.70	113 32.90	0041.0	979404.30	-32.40
0082	31 21.37	113 33.10	0035.0	979409.87	-33.10
0083	31 21.90	113 33.20	0045.0	979409.28	-33.20
0084	31 22.31	113 33.60	0049.0	979410.04	-33.20
0085	31 22.82	113 33.80	0044.0	979409.77	-34.60
0086	31 23.30	113 34.00	0042.0	979409.30	-35.80
0087	31 23.80	113 34.30	0044.0	979408.58	-37.10
0088	31 24.25	113 34.70	0042.0	979408.29	-41.10
0089	31 24.71	113 34.90	0041.0	979409.76	-38.20
0090	31 25.17	113 35.20	0036.0	979409.51	-38.30
0091	31 25.68	113 35.50	0026.0	979411.20	-37.70
0092	31 26.15	113 35.80	0027.0	979412.40	-37.40
0093	31 26.47	113 36.20	0020.0	979413.69	-37.00
0094	31 26.87	113 36.60	0016.0	979414.37	-37.00
0095	31 27.32	113 36.80	0018.0	979413.64	-37.60
0096	31 28.16	113 37.40	0019.0	979413.24	-39.60
0097	31 28.68	113 37.80	0017.0	979414.89	-38.90
0098	31 29.17	113 38.10	0018.0	979416.98	-37.40

Reproduced with permission of the copyright owner. Further reproduction prohibited without permission.

STATION	LATITUDE (DEG,MIN)	LONGITUDE (DEG,MIN)	ELEV. (FT)	OBS. GRAV. (MGAL)	B.A. (MGAL)
C099	31 30.60	113 38.80	0021.0	979419.12	-37.00
0100	31 26.87	113 35.50	0045.0	979413.57	-36.20
0101	31 26.26	113 34.70	0060.0	979411.75	-36.20
C102	31 25.70	113 33.80	0070.0	979409.05	-37.50
C103	31 25.17	113 33.10	0080.0	979407.73	-37.50
0104	31 24.06	113 32.60	0075.0	979407.38	-36.70
0105	31 22.45	113 32.60	0065.0	979405.24	-37.30
0106	31 21.90	113 31.80	0060.0	979401.64	-40.50
C107	31 21.60	113 30.90	0075.0	979399.63	-41.20
0108	31 29.00	113 25.00	0175.0	979414.20	-30.50
0109	31 28.90	113 24.70	0170.0	979413.89	-32.40
0110	31 28.78	113 21.90	0175.0	979416.26	-29.70
0111	31 28.62	113 29.10	C230.0	979424.57	-17.70
0112	31 28.65	113 22.00	0210.0	979418.43	-25.10
C113	31 47.40	113 17.40	0540.0	979407.88	-39.60
0114	31 48.18	113 17.00	0569.0	979406.87	-39.80
0115	31 48.65	113 16.80	0585.0	979406.92	-39.50
0116	31 49.40	113 16.40	0604.0	979407.69	-38.70
0117	31 50.04	113 15.80	0630.0	979407.52	-38.00
0118	31 50.75	113 15.30	0650.0	979406.08	-39.30
0119	31 51.50	113 14.90	0670.0	979407.72	-37.50
C120	31 52.76	113 14.70	0670.0	979407.06	-39.80
0121	31 51.87	113 14.75	0663.0	979405.22	-39.90
C122	31 52.10	113 14.70	0666.0	979405.71	-40.50
C123	31 52.40	113 15.00	0665.0	979405.28	-41.40
0124	31 52.54	113 15.50	0660.0	979404.29	-42.90
C125	31 52.35	113 14.40	0675.0	979406.10	-39.90
0126	31 52.80	113 14.30	0680.0	979402.27	-44.10
0127	31 52.54	113 14.30	0678.0	979403.58	-42.50
0128	31 52.79	113 16.50	0660.0	979407.13	-40.40
0129	31 53.10	113 17.50	0640.0	979409.25	-39.90
C130	31 50.76	113 20.40	0640.0	979409.92	-36.00
0131	31 50.82	113 20.80	0641.0	979405.64	-39.80
0132	31 51.44	113 21.20	0680.0	979405.34	-39.20
0133	31 51.70	113 21.80	0831.0	979401.64	-40.20
0134	31 51.70	113 22.90	0831.0	979398.77	-41.00
C135	31 51.51	113 23.90	0863.0	979391.81	-44.40
0136	31 51.45	113 24.70	0901.0	979388.43	-43.50
0137	31 51.87	113 24.90	0938.0	979386.80	-44.50
0138	31 52.14	113 25.61	1006.0	979383.04	-42.80
0139	31 49.54	113 16.90	0590.0	979408.98	-38.40
C140	31 50.28	113 16.70	0609.0	979409.45	-37.70
0141	31 51.17	113 16.60	0630.0	979409.23	-37.90
C142	31 51.94	113 17.00	0640.0	979409.40	-38.20
0143	31 52.15	113 14.40	0665.0	979406.25	-40.10
0144	31 43.20	113 18.80	0436.0	979419.77	-28.20
0145	31 43.23	113 19.30	0437.0	979474.22	-28.60
C146	31 43.20	113 19.70	0413.0	979420.77	-28.60
0147	31 43.41	113 20.10	0411.0	979420.19	-29.60
0148	31 43.71	113 20.30	0423.0	979419.72	-29.80
0149	31 44.06	113 20.60	0437.0	979418.33	-30.30
0150	31 44.47	113 20.90	0451.0	979417.41	-31.00

Reproduced with permission of the copyright owner. Further reproduction prohibited without permission.

STATION	LATITUDE (DEG,MIN)	LONGITUDE (DEG,MIN)	ELEV. (FT)	OBS. GRAV. (MGAL)	B.A. (MGAL)
0151	31 45.06	113 21.60	0484.0	979416.35	-30.70
0151	31 41.75	113 17.70	0414.0	979418.50	-28.90
0153	31 41.70	113 14.50	0505.0	979414.17	-27.50
1001	31 55.55	112 58.20	1314.0	979363.90	-57.52
1002	31 55.80	112 59.30	1157.0	979363.93	-57.80
1003	31 56.15	113 00.30	1117.0	979368.00	-57.20
1004	31 56.45	113 01.20	1067.0	979371.46	-56.50
1005	31 56.65	113 01.80	1039.0	979371.67	-58.30
1006	31 56.75	113 02.30	1011.0	979373.13	-58.60
1007	31 57.15	113 03.60	0964.0	979379.18	-55.70
1008	31 51.00	113 03.00	0973.0	979377.05	-56.80
1009	31 57.30	113 04.20	0961.0	979380.08	-54.90
1010	31 57.50	113 04.80	0973.0	979380.86	-54.20
1011	31 57.60	113 04.80	0973.0	979380.99	-54.20
1012	31 57.80	113 05.90	0994.0	979374.36	-59.90
1013	31 57.70	113 05.40	0977.0	979379.53	-55.60
1014	31 58.00	113 06.40	1001.0	979371.65	-62.40
1015	31 58.55	113 08.20	1066.0	979373.46	-57.40
1016	31 53.30	113 09.20	1084.0	979377.33	-52.10
1017	31 58.35	113 09.90	0994.0	979385.79	-49.10
1018	31 58.45	113 10.60	0940.0	979391.57	-46.70
1019	31 58.60	113 11.60	0891.0	979391.73	-49.70
1020	31 58.75	113 12.70	0850.0	979394.68	-51.20
1021	31 58.80	113 13.80	0824.0	979399.59	-49.20
1022	31 59.00	113 14.80	0775.0	979403.64	-45.40
1023	31 59.15	113 16.30	0742.0	979410.06	-41.10
1024	31 59.30	113 17.50	0721.0	979411.26	-41.40
1025	31 59.50	113 19.00	0690.0	979416.58	-38.20
1026	31 59.65	113 19.90	0665.0	979417.72	-38.80
1027	32 02.69	113 32.80	0728.0	979416.00	-40.80
1028	32 02.55	113 33.60	0724.0	979416.95	-39.80
1029	32 02.50	113 33.90	0754.0	979409.43	-45.50
1030	32 02.46	113 34.20	0800.0	979405.43	-46.70
1031	32 02.00	113 34.30	1105.0	979379.27	-53.90
1032	32 01.78	113 32.90	0729.0	979413.27	-42.20
1033	32 01.30	113 33.60	0723.0	979410.56	-44.60
1034	32 01.11	113 34.00	0729.0	979409.20	-45.40
1035	32 00.83	113 34.40	0938.0	979407.58	-46.10
1036	32 00.00	113 21.30	0659.0	979421.55	-35.40
1037	32 00.06	113 21.50	0652.0	979421.57	-35.90
1038	32 00.15	113 21.80	0685.1	979420.76	-36.90
1044	32 03.07	113 31.90	0760.0	979412.76	-42.60
1045	32 03.49	113 31.70	0772.0	979410.17	-45.02
1046	32 03.87	113 31.80	0783.0	979410.79	-44.20
1047	32 04.20	113 31.90	0794.0	979413.33	-41.50
1048	32 04.51	113 32.20	0802.0	979412.76	-42.01
1049	32 04.75	113 32.60	0801.0	979412.74	-42.40
1050	32 04.89	113 33.10	0794.0	979415.27	-40.50
1051	32 05.00	113 33.50	0784.0	979416.79	-39.70
1052	32 04.93	113 33.90	0770.0	979415.25	-42.00
1053	32 04.95	113 34.20	0765.0	979415.05	-42.50
1054	32 04.95	113 34.60	0762.0	979415.10	-42.80

Reproduced with permission of the copyright owner. Further reproduction prohibited without permission.

STATION	LATITUDE (DEG,MIN)	LONGITUDE (DEG,MIN)	ELEV. (FT)	OBS. GRAV. (MGAL)	B.A. (MGAL)
1055	32 04.97	113 35.10	0772.0	979418.48	-38.70
1056	32 05.02	113 35.60	0783.0	979414.31	-42.30
1057	32 05.15	113 36.10	0790.0	979413.09	-43.30
1058	32 05.25	113 36.50	0804.0	979410.73	-44.90
1059	32 05.24	113 37.00	0819.0	979408.79	-45.60
1060	32 05.19	113 37.50	0838.0	979406.45	-47.10
1061	32 04.67	113 41.00	0835.0	979405.46	-47.50
1062	31 55.48	113 22.20	0681.0	979412.31	-37.00
1063	31 55.65	113 23.00	0692.0	979412.48	-36.70
1064	31 55.77	113 23.80	0741.0	979410.14	-34.90
1065	31 55.62	113 24.30	0764.0	979410.21	-34.60
1066	31 55.21	113 25.20	0811.0	979404.37	-37.0
1067	31 54.77	113 25.70	0851.0	979400.30	-38.10
1068	31 54.66	113 26.50	0886.0	979397.47	-38.70
1069	31 55.19	113 26.90	0873.0	979392.79	-39.90
1070	31 55.52	113 27.00	0862.0	979394.67	-38.60
1071	31 56.40	113 27.20	0886.0	979393.46	-39.00
1072	31 57.04	113 26.70	0873.0	979399.64	-40.50
1073	31 57.76	113 26.30	0822.0	979401.43	-42.80
1074	31 58.70	113 26.30	0805.0	979402.11	-44.60
1075	31 59.62	113 25.60	0779.0	979406.61	-42.70
1076	32 00.28	113 25.60	0776.0	979408.19	-42.10
1077	31 46.30	113 17.20	0425.0	979419.85	-32.10
1078	31 46.40	113 15.30	0477.0	979414.79	-34.10
1079	31 47.85	113 12.70	0560.0	979408.25	-37.70
1080	31 48.20	113 11.70	0598.0	979406.10	-38.60
1081	31 47.70	113 06.90	0749.0	979388.11	-47.50
1082	31 44.00	113 04.20	0901.0	979371.04	-49.20
1083	31 45.40	113 01.00	1143.0	979351.52	-56.10
1084	31 48.75	112 12.90	1475.0	979332.56	-59.70
1085	31 50.15	112 11.30	1370.0	979336.68	-63.80
2001	31 20.30	113 33.20	0032.0	979409.93	-31.65
2002	31 20.20	113 33.80	0030.0	979412.50	-29.07
2003	31 19.90	113 34.90	0028.0	979415.41	-25.87
2004	31 21.40	113 39.90	0037.0	979422.74	-33.43
2005	31 22.10	113 40.80	0050.0	979420.96	-35.38
2006	31 22.90	113 41.70	0053.0	979422.23	-35.01
2007	31 33.70	113 42.70	0063.0	979422.81	-34.91
2008	31 34.50	113 43.30	0070.0	979424.47	-33.91
2009	31 35.30	113 44.10	0063.0	979429.43	-30.45
2010	31 35.70	113 44.50	0080.0	979429.86	-29.54
2011	31 36.60	113 45.30	0070.0	979430.24	-30.97
2012	31 37.40	113 46.40	0068.0	979430.87	-31.54
2013	31 37.80	113 47.70	0072.0	979428.50	-34.21
2014	31 37.90	113 48.80	0055.0	979428.44	-35.42
2015	31 37.80	113 49.50	0046.0	979427.21	-37.06
2016	31 37.90	113 50.00	0044.0	979426.25	-38.27
2017	31 38.00	113 51.20	0050.0	979424.99	-39.31
2018	31 39.30	113 52.20	0048.0	979426.33	-38.49
2019	31 39.20	113 53.30	0065.0	979427.53	-37.49
2020	31 40.00	113 54.00	0081.0	979429.43	-35.61

Reproduced with permission of the copyright owner. Further reproduction prohibited without permission.

STATION	LATITUDE (DEG,MIN)	LONGITUDE (DEG,MIN)	ELEV. (FT)	OBS. GRAV. (MGAL)	B.A. (MGAL)
2021	31 41.00	113 54.80	0066.0	979431.30	-35.94
2022	31 42.10	113 56.20	0081.0	979431.29	-36.58
2023	31 37.20	113 45.70	0076.0	979431.80	-29.86
2024	31 37.80	113 45.30	0097.0	979467.03	-26.78
2025	31 38.60	113 45.10	0114.0	979434.37	-26.90
2026	31 20.00	113 36.20	0029.0	979416.45	-24.82
2027	31 19.40	113 36.40	0020.0	979418.82	-22.27
2028	31 19.40	113 36.80	0027.0	979423.10	-17.57
2029	31 19.90	113 36.90	0030.0	979420.08	-21.08
2030	31 20.30	113 37.70	0023.0	979423.58	-18.54
2031	31 18.50	113 32.40	0015.0	979414.49	-25.57
3002	31 41.72	113 06.50	238.0	979383.44	-41.03
3003	31 40.12	113 05.40	0253.0	979378.42	-42.32
3004	31 38.40	113 06.00	290.0	979372.64	-38.58
3005	31 39.28	113 06.20	265.0	979380.73	-36.54
3006	31 40.17	113 06.50	240.0	979381.88	-41.45
3007	31 42.30	113 08.20	215.0	979391.49	-39.51
3008	31 42.65	113 09.00	210.0	979393.57	-38.99
3009	31 42.90	113 10.10	198.0	979393.79	-41.45
3010	31 43.10	113 10.70	195.0	979398.72	-37.32
1079A	31 42.90	113 12.60	175.0	979409.27	-30.47
3011	31 43.25	113 13.40	175.0	979407.26	-31.93
3012	31 42.20	113 13.70	160.0	979413.71	-27.96
3013	31 41.36	113 23.00	419.0	979419.42	-27.18
3014	31 41.86	113 23.70	491.0	979417.37	-25.58
3015	31 42.36	113 24.70	623.0	979409.88	-25.83
3016	31 42.48	113 25.20	662.0	979406.55	-26.98
3017	31 40.90	113 22.30	395.0	979420.44	-26.98
3018	31 40.30	113 21.30	380.0	979420.09	-27.41
3019	31 40.10	113 20.30	388.0	979418.96	-27.80
3020	31 42.74	113 15.00	505.0	979415.45	-27.85
3021	31 43.29	113 15.90	502.0	979418.84	-25.38
3022	31 44.22	113 16.10	523.0	979413.61	-30.61
3023	31 44.48	113 16.20	526.0	979412.81	-31.58
3024	31 45.38	113 16.00	542.0	979410.78	-33.86
3025	31 46.20	113 15.70	558.0	979408.28	-36.51
3026	31 46.97	113 15.20	577.0	979405.90	-38.79
3027	41 47.70	113 14.80	598.0	979405.39	-39.03
3028	31 48.75	113 14.20	614.0	979406.07	-38.80
3029	31 49.55	113 14.40	629.0	979406.29	-38.76
3030	31 50.45	113 14.70	655.0	979405.07	-39.54
3031	31 51.30	113 14.60	671.0	979404.45	-40.35
3032	31 51.75	113 14.10	687.0	979404.42	-40.02
3033	31 57.60	113 38.3	690.0	979413.78	-41.38
3034	31 58.20	113 39.10	655.0	979413.99	-41.08
3035	31 58.45	113 40.00	622.0	979413.74	-43.55
3036	31 57.80	113 40.30	601.0	979420.21	-37.56
3037	31 57.60	113 40.30	587.0	979418.08	-40.26
3038	31 57.80	113 40.70	580.0	979417.66	-41.37
3039	31 57.15	113 40.90	545.0	979416.74	-43.51
3040	31 56.35	113 41.20	505.0	979419.51	-42.06
3041	31 55.80	113 42.00	455.0	979422.83	-41.00

Reproduced with permission of the copyright owner. Further reproduction prohibited without permission.

STATION	LATITUDE (DEG,MIN)	LONGITUDE (DEG,MIN)	ELEV. (FT)	OBS. GRAV. (MGAL)	B.A. (MGAL)
3042	31 55.75	113 43.10	435.0	979424.22	-40.74
3043	31 55.CC	113 43.40	415.0	979423.89	-41.26
3044	31 54.20	113 43.90	400.0	979426.79	-38.18
3045	31 55.25	113 41.80	477.0	979419.66	-42.11
3046	31 55.0C	113 40.80	517.0	979417.16	-41.87
3047	31 54.75	113 40.20	554.0	979414.16	-42.31
3048	31 55.0C	113 39.80	548.0	979414.54	-42.63
3049	31 54.75	113 39.10	625.0	979410.74	-41.47
3050	31 55.4C	113 38.20	645.0	979413.01	-38.88
3051	31 55.8C	113 37.40	682.0	979416.31	-33.90
3052	31 55.9C	113 36.60	724.0	979410.24	-37.58
3053	31 39.4C	113 45.10	135.0	979432.84	-28.15
3054	31 4C.35	113 45.00	143.0	979432.40	-29.40
3055	31 41.2C	113 45.00	165.0	979431.87	-29.75
3056	31 41.70	113 45.00	171.0	979429.87	-32.07
3057	31 42.15	113 44.60	181.0	979428.20	-33.74
3058	31 42.90	113 44.10	206.0	979424.73	-36.73
3059	31 43.50	113 43.70	214.0	979423.96	-37.82
3060	31 44.15	113 43.20	220.0	979426.21	-36.09
3061	31 44.70	113 42.60	230.0	979427.84	-34.60
3062	31 31.90	113 43.00	0020.0	979415.79	-42.07
3063	31 32.75	113 42.90	0023.0	979419.10	-39.72
3064	31 33.20	113 43.40	0036.0	979418.46	-40.18
3065	31 4C.0C	113 17.80	405.0	979417.15	-28.45
3066	31 39.18	113 18.10	393.0	979418.48	-26.79
3067	31 38.25	113 18.10	379.0	979418.96	-25.9
3068	31 37.43	113 18.10	366.0	979421.11	-23.42
3069	31 36.66	113 17.80	352.0	979419.74	-24.6
3070	31 35.93	113 17.50	332.0	979417.88	-26.68
3071	31 35.20	113 17.50	314.0	979414.78	-29.87
3072	31 34.30	113 17.60	303.0	979411.57	-32.53
3073	31 35.77	113 18.70	319.0	979416.98	-28.14
3074	31 36.40	113 19.60	320.0	979420.53	-25.38
3075	31 36.85	113 20.30	331.0	979420.52	-25.33
3076	31 38.C6	113 21.50	346.0	979419.84	-26.74
3077	31 38.16	113 22.40	350.0	979421.22	-25.66
3078	31 38.27	113 24.40	331.0	979423.75	-24.01
3080	31 38.52	113 25.20	355.0	979423.96	-22.70
3081	31 38.8C	113 26.00	367.0	979425.07	-21.25
3082	31 39.3C	113 26.70	0420.0	979421.15	-22.61
3083	31 35.0C	113 22.40	0281.0	979425.76	-20.60
3085	31 35.28	113 23.20	0271.0	979433.66	-13.68
3087	31 35.80	113 25.00	0275.0	979436.16	-11.64
3088	31 35.95	113 24.40	0275.0	979433.73	-14.27
3089	31 35.56	113 25.40	0289.0	979436.67	-09.97
3090	31 35.27	113 25.80	0320.0	979433.28	-11.11
3086	31 35.55	113 24.00	0273.0	979433.17	-14.41
3084	31 35.13	113 22.80	0270.0	979429.43	-18.77
3091	31 27.60	113 22.10	0155.0	979410.80	-33.49
3092	31 27.6C	113 19.40	0212.0	979421.46	-19.14
3093	31 26.7C	113 19.5C	0200.0	979417.62	-22.49
3094	31 25.90	113 20.0C	0190.0	979411.89	-27.75

Reproduced with permission of the copyright owner. Further reproduction prohibited without permission.

STATION	LATITUDE (DEG,MIN)	LONGITUDE (DEG,MIN)	ELEV. (FT)	OBS. GRAV. (MGAL)	B.A. (MGAL)
3095	31 27.30	113 18.20	0235.0	979432.06	-07.43
3096	31 27.30	113 17.50	0249.0	979432.68	-05.30
3097	31 26.70	113 16.70	0267.0	979432.80	-03.29
3098	31 27.40	113 16.40	0267.0	979426.95	-10.08
3099	31 27.80	113 15.40	0287.0	979419.51	-16.86
3100	31 25.20	113 15.50	0295.0	979425.22	-07.17
3101	31 24.40	113 14.80	0294.0	979422.34	-09.04
3102	31 23.70	113 14.40	0280.0	979418.03	-13.25
3103	31 22.10	113 13.30	0255.0	979406.35	-24.27
3104	31 20.50	113 12.40	0195.0	979407.57	-24.50
3105	31 18.80	113 11.30	0145.0	979408.62	-24.32
3106	31 17.50	113 10.60	0120.0	979407.80	-24.89
3107	31 18.00	113 10.00	0160.0	979409.65	-21.31
3108	31 18.80	113 09.30	0270.0	979407.75	-17.69
3109	31 19.70	113 08.80	0400.0	979399.39	-19.46
3110	31 21.10	113 07.40	0640.0	979388.64	-17.54
3111	31 24.00	113 06.80	0595.0	979388.98	-23.80
3112	31 16.30	113 12.00	0052.0	979403.76	-31.39
3113	31 15.50	113 12.70	0015.0	979400.52	-35.78
3114	31 14.60	113 12.40	0015.0	979398.58	-36.51
3115	31 13.70	113 12.20	0015.0	979397.87	-36.91
3116	31 15.80	113 10.70	0073.0	979401.96	-31.26
3117	31 15.10	113 09.40	0064.0	979401.81	-31.01
3118	31 17.20	113 13.30	0044.0	979404.27	-32.57
3119	31 17.60	113 14.50	0037.0	979404.45	-33.35
3120	31 18.00	113 15.70	0027.0	979404.37	-34.57
3121	31 18.20	113 16.80	0047.0	979404.40	-33.61
3122	31 18.50	113 18.20	0050.0	979406.36	-31.87
3123	31 18.70	113 19.40	0060.0	979408.00	-29.90
3124	31 18.90	113 20.60	0058.0	979408.92	-29.37
3125	31 19.30	113 22.80	0062.0	979409.16	-29.43
3126	31 19.50	113 23.80	0062.0	979412.82	-26.04
3127	31 19.40	113 25.20	0047.0	979405.10	-34.52
3128	31 18.50	113 25.10	0045.0	979405.62	-32.91
3129	31 17.90	113 24.30	0040.0	979408.40	-29.63
3130	31 17.40	113 23.50	0030.0	979412.21	-25.74
3131	31 19.40	113 26.80	0056.0	979402.09	-36.99
3132	31 19.20	113 28.40	0036.0	979400.08	-39.93
3133	31 18.80	113 30.00	0029.0	979402.83	-37.07
3134	31 18.65	113 30.70	0027.0	979406.45	-33.36
3135	31 18.40	113 31.20	0025.0	979410.90	-28.97
3136	31 21.70	113 33.70	0045.0	979410.39	-32.30
3137	31 22.10	113 34.70	0040.0	979411.89	-31.63
3138	31 22.25	113 35.80	0030.0	979413.87	-30.46
3139	31 22.20	113 36.80	0020.0	979415.80	-29.06
3140	31 23.20	113 37.00	0025.0	979419.01	-26.89
3141	31 21.50	113 42.20	0020.0	979418.77	-38.55
3142	31 20.90	113 41.20	0020.0	979421.78	-34.73
3143	31 20.60	113 40.20	0015.0	979422.97	-33.44
3144	31 29.90	113 40.60	0015.0	979419.46	-36.96
3145	31 29.15	113 38.90	0015.0	979417.20	-38.21
3146	31 28.15	113 35.70	0055.0	979411.25	-39.21

Reproduced with permission of the copyright owner. Further reproduction prohibited without permission.

STATION	LATITUDE (DEG:MIN)	LONGITUDE (DEG:MIN)	ELEV. (FT)	OBS. GRAV. (MGAL)	B.A. (MGAL)
3147	31 45.25	113 22.60	0550.0	979418.24	-25.75
3148	31 45.70	113 23.40	0597.0	979415.00	-26.78
3149	31 46.05	113 24.30	0719.0	979406.32	-28.61
3150	31 46.15	113 25.00	0821.0	979399.76	-29.18
3151	31 46.15	113 25.80	1051.0	979383.20	-31.94
3152	31 46.30	113 26.00	1190.0	979367.65	-34.15
3153	31 46.60	113 27.70	1790.0	979333.39	-36.02
5040	32 17.60	114 09.60	0744.0	979429.70	-46.30
5041	32 17.30	114 08.60	0775.6	979430.27	-43.43
5042	32 16.80	114 07.50	0802.2	979433.54	-37.88
5043	32 16.15	114 06.70	0819.2	979432.83	-36.68
5044	32 15.50	114 05.90	0822.0	979433.28	-35.18
5045	32 15.10	114 05.30	0828.2	979435.53	-32.02
5046	32 14.80	114 04.80	0863.4	979433.18	-31.84
5047	32 14.30	114 03.00	0898.5	979428.85	-33.39
5048	32 14.60	114 03.90	0881.4	979431.42	-32.26
5050	32 13.25	114 01.20	0935.7	979426.06	-32.52
5051	32 12.50	114 00.40	0879.5	979429.36	-32.57
5052	32 11.30	113 59.30	0878.3	979425.08	-34.97
5053	32 11.30	113 58.50	0947.6	979420.86	-34.36
5054	32 10.90	113 57.90	1049.9	979414.24	-34.28
5055	32 10.30	113 57.20	1109.1	979408.80	-35.36
5056	32 09.70	113 56.80	1186.6	979403.88	-34.83
5057	32 08.90	113 56.00	1195.1	979402.11	-35.00
5058	32 08.60	113 55.30	1235.2	979397.22	-37.08
5059	32 08.20	113 54.30	1234.6	979393.34	-40.45
5060	32 07.70	113 53.50	1139.3	979397.11	-41.73
5061	32 07.40	113 52.60	1031.9	979402.14	-42.73
5062	32 07.20	113 51.70	0907.4	979408.76	-43.32
5063	32 07.15	113 50.80	0846.3	979410.80	-44.87
5064	32 07.10	113 49.90	0846.7	979408.25	-47.33
5065	32 07.00	113 49.00	0877.4	979407.49	-46.11
5066	32 07.00	113 48.00	0900.9	979409.02	-43.17
5067	32 06.85	113 47.00	0931.2	979409.77	-40.41
5068	32 06.70	113 46.10	0988.8	979405.40	-41.12
5070	32 05.80	113 44.50	0980.3	979403.78	-42.03
5071	32 05.30	113 43.80	0927.0	979405.28	-43.06
5072	32 04.70	113 43.20	0857.6	979407.84	-43.85
5073	32 04.30	113 42.50	0806.6	979409.88	-44.34
5074	32 04.50	113 41.40	0814.9	979408.89	-45.09
5075	32 04.50	113 40.70	0841.6	979406.35	-46.04
5076	32 04.10	113 40.00	0820.1	979408.15	-44.98
5077	32 03.80	113 39.00	0819.3	979408.78	-43.99
5078	32 03.60	113 38.20	0796.6	979411.45	-42.41
5079	32 30.50	113 37.20	0780.9	979413.17	-41.53
5080	32 03.50	113 36.30	0752.2	979413.92	-42.48
5081	32 03.30	113 35.30	0746.2	979413.23	-43.26
5082	32 03.20	113 34.30	0738.7	979413.03	-45.77
5083	32 02.90	113 33.80	0757.2	979413.06	-42.22
5084	32 02.71	113 32.50	0745.9	979415.65	-40.06
5085	32 02.55	113 31.50	0771.9	979412.47	-41.52
5086	32 02.60	113 30.30	0797.5	979407.88	-44.58

Reproduced with permission of the copyright owner. Further reproduction prohibited without permission.

STATION	LATITUDE (DEG,MIN)	LONGITUDE (DEG,MIN)	ELEV. (FT)	OBS. GRAV. (MGAL)	B.A. (MGAL)
5087	32 02.73	113 29.20	0775.2	979406.73	-47.25
5088	32 02.68	113 28.20	0776.4	979402.60	-51.24
5089	32 02.30	113 27.40	0777.8	979400.04	-53.20
5090	32 02.00	113 26.10	0746.0	979405.89	-48.85
5091	32 01.60	113 25.20	0732.5	979409.58	-45.43
5092	32 01.25	113 24.20	0757.5	979412.86	-40.18
5093	32 01.00	113 23.50	0713.5	979417.83	-37.51
5094	32 00.70	113 22.60	0699.5	979418.08	-37.70
5095	32 00.15	113 21.80	0685.1	979420.76	-35.13
5096	31 59.75	113 29.80	0680.1	979421.02	-34.63
5097	31 59.50	113 19.60	0697.0	979416.30	-38.00
5098	31 59.30	113 18.50	0715.6	979413.73	-39.18
5099	31 59.20	113 17.40	0742.9	979411.33	-39.82
5100	31 59.10	113 16.20	0767.9	979409.11	-40.40
5101	31 58.90	113 15.00	0797.7	979403.43	-44.02
5102	31 58.85	113 13.90	0826.6	979398.77	-46.88
5103	31 58.70	113 12.80	0882.5	979393.64	-48.45
5104	31 58.50	113 11.70	0956.3	979392.18	-45.21
5105	31 58.30	113 10.50	0996.7	979390.10	-44.60
5106	31 58.20	113 09.50	1084.7	979380.93	-48.36
5107	31 58.20	113 08.70	1077.7	979376.92	-52.79

Reproduced with permission of the copyright owner. Further reproduction prohibited without permission.